Available online at www.sciencedirect.com

SCIENCE DIRECT

Developmental Biology 294 (2006) 203–219

DEVELOPMENTAL BIOLOGY

www.elsevier.com/locate/ydbio

Evi1 is specifically expressed in the distal tubule and duct of the *Xenopus* pronephros and plays a role in its formation

Claude Van Campenhout [a], Massimo Nichane [a], Aline Antoniou [a], Hélène Pendeville [b], Odile J. Bronchain [c], Jean-Christophe Marine [d], Andre Mazabraud [c], Marianne L. Voz [b], Eric J. Bellefroid [a,*]

[a] *Laboratoire d'Embryologie Moléculaire, Université Libre de Bruxelles, Institut de Biologie et de Médecine Moléculaires (IBMM), rue des Profs. Jeener et Brachet 12, B-6041 Gosselies, Belgium*

[b] *Laboratoire de Biologie Moléculaire et Génie Génétique, Institut de Chimie, Université de Liege, Bâtiment B6, 4000, Liège (Sart-Tilman), Belgium*

[c] *Transgenèse et Génétique des Amphibiens, CNRS UMR 8080, IBAIC, Université Paris-Sud, bât. 447, F-91405 Orsay Cedex, France*

[d] *Laboratory for Molecular Cancer Biology, Flanders Interuniversity Institute for Biotechnology (VIB), University of Ghent, B-9052 Ghent, Belgium*

Received for publication 13 June 2005; revised 13 February 2006; accepted 23 February 2006
Available online 30 March 2006

Abstract

The *ecotropic viral integration site 1* (*Evi1*) and related *MEL1* (*MDS1*/*Evi1*-like gene 1) genes are zinc finger oncogenic transcription factors involved in myeloid leukaemia. Here, we show that in *Xenopus*, *Evi1* and *MEL1* have partially overlapping restricted embryonic expression profiles. Within the pronephros, *Evi1* and *MEL1* are sequentially expressed within the distal tubule and duct compartments, *Evi1* transcription being detected prior to any sign of pronephric morphogenesis. In the pronephros of zebrafish embryos, *Evi1* expression is restricted to the posterior portion of the duct, the anterior portion having characteristics of proximal tubules. In the *Xenopus* pronephros, *Evi1* expression is upregulated by retinoid signaling and repressed by overexpression of *xWT1* and by Notch signaling. Overexpression of *Evi1* from late neurula stage specifically inhibits the expression of proximal tubule and glomus pronephric markers. We show that the first zinc finger and CtBP interaction domains are required for this activity. Overexpression of a hormone-inducible *Evi1-VP16* antimorphic fusion with activation at neurula stage disrupts distal tubule and duct formation and expands the expression of glomus markers. Although overexpression of this construct also causes in many embryos a reduction of proximal tubule markers, embryos with expanded and ectopic staining have been also observed. Together, these data indicate that Evi1 plays a role in the proximo-distal patterning of the pronephros and suggest that it may do so by functioning as a CtBP dependent repressor.

Keywords: *Evi1*; *MEL1*; Zinc finger; Notch; Pronephros; *Xenopus laevis*; Zebrafish; Chicken

Introduction

In vertebrates, a succession of three different nephric systems, the pronephros, mesonephros and metanephros, is used to dispose off waste and control water balance during development and adult life. All three vertebrate kidneys consist of a basic functional unit, the nephron, but differ with respect to the number and organization of the nephrons within the kidney. The pronephros is the first kidney to form in embryos of all vertebrate species and is the functional embryonic kidney of amphibian and fish embryos. In higher vertebrates, the pronephros is a rudimentary organ and the first functional kidney is the mesonephros. The pronephros is a paired organ that consists in a single non-integrated nephron found in lateral position of the embryo. Three components form the functional pronephros: (i) the glomus, which is the site of blood filtration (ii) the tubules, where filtrate resorption occurs, and (iii) the nephric duct, which carries the urine to the exterior. The simplicity of this organ coupled to the fact that it displays the same basic organization as the more evolved mesonephros and metanephros makes this an attractive model to study the earliest events of kidney organogenesis (Brändli, 1999; Vize et al., 2003).

* Corresponding author. Fax: +32 2 650 97 33.
E-mail address: ebellefr@ulb.ac.be (E.J. Bellefroid).

0012-1606/$ - see front matter © 2006 Elsevier Inc. All rights reserved.
doi:10.1016/j.ydbio.2006.02.040

Studies of pronephros development are currently mainly conducted in the frog, *Xenopus laevis*, and in the zebrafish, *Danio rerio*, due to the unique advantages those experimental systems offer for studies of organogenesis (Ryffel, 2003; Jones, 2005; Drummond, 2005). In both species, the pronephric kidney contains two tubular components, the pronephric tubules and duct. In amphibians, the pronephros contains a three branched tubule domain terminated by ciliated nephrostomes that connect the tubules to the coelom where blood filtrate is delivered by the glomus. This tubule domain which appears in the anterior intermediate mesoderm is prolonged by the duct which runs more posteriorly along the side of the tadpole embryo. In zebrafish, the short tubule that projects laterally from the fused glomeruli at the midline has only one branch and thus forms an apparent continuous structure with the pronephric duct which runs caudally to the cloaca (Vize et al., 1997; Drummond, 2003). In the frog, distinct domains and subdomains within the tubules and duct compartments have been recently defined based on the localized expression of various membrane transporter genes (Zhou and Vize, 2004). However, the segmentation of the zebrafish nephron has been much less studied. The glomerulus, tubule and duct segments have been defined based solely on the expression of a few early transcription factors (Serluca and Fishman, 2001). The degree of similarity of the compartmentalization of the zebrafish and *Xenopus* pronephros is thus still not yet clear.

All three components of the pronephros develop within the intermediate mesoderm in response to signals from the anterior somites, lateral plate and surface ectoderm (Seufert et al., 1999; Mauch et al., 2000; James and Schultheiss, 2003). Studies in chicken have shown that BMP signaling plays a particularly important role in the establishment of the intermediate mesoderm (Obara-Ishihara et al., 1999; James and Schultheiss, 2005). Retinoic acid (RA), which has proven to be necessary for proper development of the vertebrate embryo, might be also important for pronephros development. First, in *Xenopus* embryos, RA treatment enhances the expression of *Xlim-1*, which is the earliest known marker of pronephric development (Taira et al., 1994; Chan et al., 2000) and expression of a dominant negative RAR blocked its expression (Blumberg et al., 1997). Second, treatment of *Xenopus* animal cap ectoderm with activin and RA induces the expression of pronephric markers (Osafune et al., 2002). In *Xenopus*, pronephric precursors are defined at early neurula stage by the combined expression of the *Pax-8* and *Xlim-1* genes, which encode critical regulators of nephric lineage specification (Carroll and Vize, 1999; Chan et al., 2000). At mid-neurula stage, the pronephric mesoderm is subdivided into two layers, the splanchnic layer (also designated medial layer) that later forms the glomus and the somatic layer (also designated lateral layer) that will give rise to the pronephros anlagen itself. At late-neurula stage, this somatic layer is further subdivided into a dorso-anterior compartment that will form the tubules and a ventro-posterior region that gives rise to the duct.

The molecular mechanisms that control the early regionalization of the pronephros are still largely unknown. Today, only a few genes are known to be involved in the proximo-distal patterning of the forming nephron. In *Xenopus*, the *xWT1* gene encoding a zinc finger transcription factor is selectively activated in the medial layer of the pronephric mesoderm. Ectopic expression of *xWT1* blocks the expression of tubule specific genes, suggesting that it may act to repress tubule-specific expression in the portion of the pronephros fated to form the glomus (Wallingford et al., 1998). In the mouse, Brn1 plays a crucial role in Henle's loop and distal tubule formation as differentiation of those compartments is severely impaired in homozygous Brn1− mutant mice (Nakai et al., 2003). Using FGF8 conditional-null allele, it has been demonstrated that FGF8 is required for the survival of cells that develop into the tubular segment (Grieshammer et al., 2005). Notch signaling has been also shown to play an important role in the early selection of cell fates within the forming nephrons favoring podocyte and proximal tubule differentiation at the expense of the duct (McLaughin et al., 2000; Cheng and Kopan, 2005; Cheng et al., 2003; Wang et al., 2003).

Here, we report our finding on the *Evi1* and *MEL1* genes. The *ecotropic viral integration site 1* (*Evi1*) and *MEL1* (*MDS1/Evi1*-like gene 1) are zinc finger proto-oncogenes that are activated by retroviral insertion or chromosome rearrangements in murine and human myelogenous leukaemia that play important roles in the normal development of haematopoietic cells and leukaemia (Morishita et al., 1988; Mucenski et al., 1988; Fichelson et al., 1992; Buonamici et al., 2004; Yuasa et al., 2005). We describe that in *Xenopus, Evi1* and *MEL1* have partially overlapping restricted embryonic expression profile. Within the pronephros, we observed that *Evi1* is activated earlier than *MEL1* prior to any overt sign of morphogenesis and that both genes are selectively expressed within the distal tubule and duct compartments. In zebrafish, we found that *Evi1* expression is restricted to the posterior region of the duct, its anterior portion having characteristics of proximal tubules. We found that in *Xenopus*, *Evi1* expression in the pronephros is regulated by xWT1, Notch and retinoid signals. We further show that ectopic activation of Evi1 at neurula stage, but not that of a first zinc finger domain or CtBP binding mutants, specifically inhibits the expression of glomus and proximal tubule markers. Conversely, inhibition of Evi1 by use of an *Evi1-VP16* antimorphic fusion disrupts distal tubule and duct and expands the expression of glomus markers. In some injected embryos, an increased and ectopic expression of proximal tubule markers could also be observed. These data thus provide the first evidence suggesting that Evi1 plays a role as a CtBP dependent repressor in the patterning of the developing pronephros.

Materials and methods

Isolation of Evi1 and MEL1 cDNAs

The full length *Evi1* and partial *MEL1* cDNA clones were isolated by screening a *Xenopus laevis* tadpole head library constructed in λZAP II (Hemmati-Brivanlou et al., 1991) using as a probe a random primed *Evi1* *Bam*H1–*Hin*dIII fragment corresponding to nucleotides 1140–3372 (a gift

from J.N. Ihle). cDNA encoding full-length zebrafish Evi1 was predicted from 5′RACE amplified cDNA, available Genbank EST sequences (CR930641, AL925638, CK679353, AL927780, AL917144) and genomic sequences. cDNA encoding full-length chicken Evi1 was predicted from available Genbank EST sequences (BU399447, BU336814, CD764994, BU328024, BU335509, BU340215, BU329315, BU336539, BU214446, BU324180).

Xenopus embryos and injections

Embryos were obtained from adult female frogs by hormone-(chorionic gonadotropin, Sigma) induced egg laying and in vitro fertilization using standard methods. *Xenopus* embryos were staged according to Nieuwkoop and Faber (1997). Capped synthetic mRNA were transcribed using the mMESSAGE mMACHINE RNA synthesis kit (Ambion). Synthetic mRNA (250 pg–2 ng) were injected in either 4-cell or 8-cell stage embryos. Nuc-LacZ mRNA (200 pg/blastomere) was used as a lineage tracer. Dexamethasone (10 μM, Sigma) was added to the growth medium at stage 18. For retinoid treatments, embryos were treated in the dark with all-trans-Retinoic Acid (Sigma) at 10 μM or all-trans-Retinal (Sigma) at 5 μM, from stages 9 to 10 at 18°C, diluted in 0.1 xMBS from 10 mM stocks in DMSO. Injected embryos were fixed 1 h in MEMFA, stained for β-galactosidase activity with 5-bromo 4-chloro-3-indolyl-β-galactopyranoside (X-Gal, Bioline) or 6-Chloro-3-indolyl-β-D-galactoside (Red-Gal, Research Organics) and stored in ethanol at −20°C. Only embryos that were phenotopically normal were scored for effect on pronephric development. The percentage of embryos with a given phenotype and the total number of embryos scored for each injection are presented in the results section. Templates for generating RNA encoding *NotchICD*, *Su(H)DBM*, *xWT1*, *xRARα1*^{405}*, *xCYP26* and *XRALDH2* have been previously described (Wettstein et al., 1997; Blumberg et al., 1997; Wallingford et al., 1998; Hollemann et al., 1998; Chen et al., 2001). Templates for *Evi1* were generated by amplifying the *Evi1* coding region (nucleotide 807 to 4017) and cloning the resulting PCR product into the *Xho*I and *Xba*I sites of the PCS2 vector. The Evi1 N-term mutant (amino acids 1–789) and Evi1 C-term mutant (amino acids 790–1055) were generated by PCR and by subcloning the resulting fragment into the *Stu*I–*Xho*I sites of pCS2-NLS-MT (Turner and Weintraub, 1994). The inducible *Evi1-hGR* was obtained by amplifying by PCR the entire coding region of *Evi1* and subcloning it into the *Stu*I and *Xho*I sites of a modified PCS2 vector in which the ligand binding domain of the human glucocorticoid receptor were inserted into the *Xho*I and *Xba*I sites (pCS2-hGR; a gift from T. Pieler). *Evi1-VP16-hGR* constructs were obtained by amplifying by PCR the entire coding region of *Evi1* and subcloning it into the *Stu*I and *Xho*I sites of a modified PCS2 vector in which the VP16 transcriptional activation domain fused to the ligand binding domain of the human glucocorticoid receptor were inserted into the *Xho*I and *Xba*I sites (pCS2-VP16-hGR; a gift from T. Pieler). The inducible mutant Evi1-ΔZF1-hGR (amino acids 264–1055) was generated by subcloning a *Nco*I–*Xho*I fragment of the *Evi1* cDNA into the *Stu*I and *Xho*I sites of the PCS2-hGR. The *Nco*I site was filled in by Klenow and codes for a Met in frame with the Evi1 construct. The Evi1-ΔZF2-hGR (deleted from amino acid 733–821) and Evi1-ΔCtBP-hGR mutants (amino acids 553–557 and 584–588) were generated by PCR and subcloning of the amplified fragment into the *Stu*I and *Xho*I sites of the PCS2-hGR vector. In the Evi1-ΔCtBP-hGR mutant, the sequences encoding residues “PFDLT” (553–557) and “PLDLS” (584–588) were replaced by site directed mutagenesis by the sequence encoding the “PFAST” and “PLAST” motifs respectively using the primers: “GGG GAA AAC AGA ATC CCC TTT GCT AGC ACT ACC AAA CG”, “CTG TTG GTA GTG CTA GCA AAG GGT GAT TCT GTT TTC CCC”, ”CAA ACC AGA TCA GCC TTT GGC TTC TAG CAT G”, “CAT GCT AGA AGC CAA AGG CTG ATC GTG GTT TG”.

RNAase protection assay

Total RNA was extracted by the NETS/phenol method and analyzed by RNAase protection assay using ^{32}P-labeled antisense probes as described previously (Krieg, 1991). RNAase protection probe for *Evi1* was generated starting from a pBluescript plasmid containing a cDNA fragment corresponding to nucleotides 286–2517 (Ihle et al., unpublished), linearizing it with *Bgl*II and transcribing it with T3. The protected fragment is 286 bases long. *EF1-* (Wettstein et al., 1997) or *FGFR* antisense probes (Ryan et al., 1998) were used as loading controls.

Whole-mount in situ hybridization

Zebrafish embryos were grown at 28°C to the desired stage and manually dechorionated. Fertilized chick eggs were grown at 37°C and staged according to Hamburger and Hamilton (1951). Zebrafish and chicken embryos were fixed overnight in 4% PFA in PBS at 4°C and stored in 100% methanol at −20°C until used. Whole-mount in situ hybridization using digoxigenin- or fluorescein-labeled antisense riboprobes in *Xenopus*, zebrafish and chicken embryos was performed as previously described with minor modifications (Harland, 1991; Wilkinson and Nieto, 1993; Broadbent and Read, 1999). Double in situ hybridization, FISH and confocal imaging were performed as previously described (Bellefroid et al., 1998; Mavropoulos et al., 2005). For sections, embryos after completion of the whole-mount procedure were gelatine-embedded and vibratome-sectioned at 30 μm thickness (Bellefroid et al., 1996).

Antisense *Evi1* riboprobe was generated from a cDNA fragment (nucleotides 1140–3372) subcloned into the *Eco*RI sites of pbKS. After linearization with Not1, the vector was transcribed with T3. *MEL1* riboprobe was generated from a 0.6-kb cDNA fragment encoding (amino acids 565–576) subcloned into pbKS. After linearization with *Xho*I, the vector was transcribed with T7. xSat1 (EST CF521505) and xPDZK1 (EST BQ731430) plasmids were linearized with Sal1 and transcribed with T7. Zebrafish Evi1 plasmid (EST AL927780) was linearized with Xho1 and transcribed with T3. Zebrafish ClC-K (EST BC053277), PDZK1 (EST BC066762) and Sat1 plasmids (EST CK240386) were linearized with EcorV and transcribed with T7. Zebrafish ret1 (EST AI793987) plasmid was linearized with Sal1 and transcribed with SP6. Chicken Evi1 (EST BU214446) plasmid was linearized with Not 1 and transcribed with T7. Those EST were obtained from the IMAGE consortium, NIBB and zebrafish EST database. Plasmids used for generating the other in situ hybridization probes were previously described: Chordin (Sasai et al., 1994), xClC-K (Vize, 2003), Xbra (Smith et al., 1991), Ep. Keratin and Sox2 (Bellefroid et al., 1998), Slug (Mayor et al., 1995), Gremlin (Hsu et al., 1998), xWT1 (Carroll and Vize, 1996), XSMP-30 (Sato et al., 2000), XPax8 (Carroll and Vize, 1999), Xlim-1 (Taira et al., 1994), X-Delta-1 (Chitnis et al., 1995), XKrox-20 (Nieto et al., 1991), Sim1 (Serluca and Fishman, 2001), EphA4 (Smith et al., 1997), nephrin (Gerth et al., 2005), c-ret (Osafune et al., 2002), GATA-3 (Zon et al., 1991).

Results

Cloning of Xenopus Evi1 and MEL1

A partial *Xenopus Evi1* cDNA clone (a gift of J. N. Ihle) was used to screen a tadpole head cDNA library (a gift from A. Hemmati-Brivanlou). A 4.4 kb cDNA was isolated and sequenced. *Evi1* orthologs in zebrafish and chicken were identified by mining the EST and genomic databases. The *Xenopus* sequence obtained encodes a predicted protein of 1054 amino acids (Accession number DQ088677) that shares 82% identity with human, 80% with murine, 80% with predicted chicken and 69% with the predicted zebrafish Evi1 protein (Fig. 1). The ten zinc fingers in all Evi1 proteins are highly conserved and share more than 90% amino acid identity. The two CtBP binding sites (“PFDLT” and “PLDLS”) and acidic domain that are present in mouse and human proteins are also conserved in the *Xenopus*, zebrafish and chicken proteins. A second partial cDNA clone was also identified in our screen that is most closely related to MEL1 (71% identity between the *Xenopus* available sequences spanning aa 565–756 and the homologous mouse sequences) (data not shown).

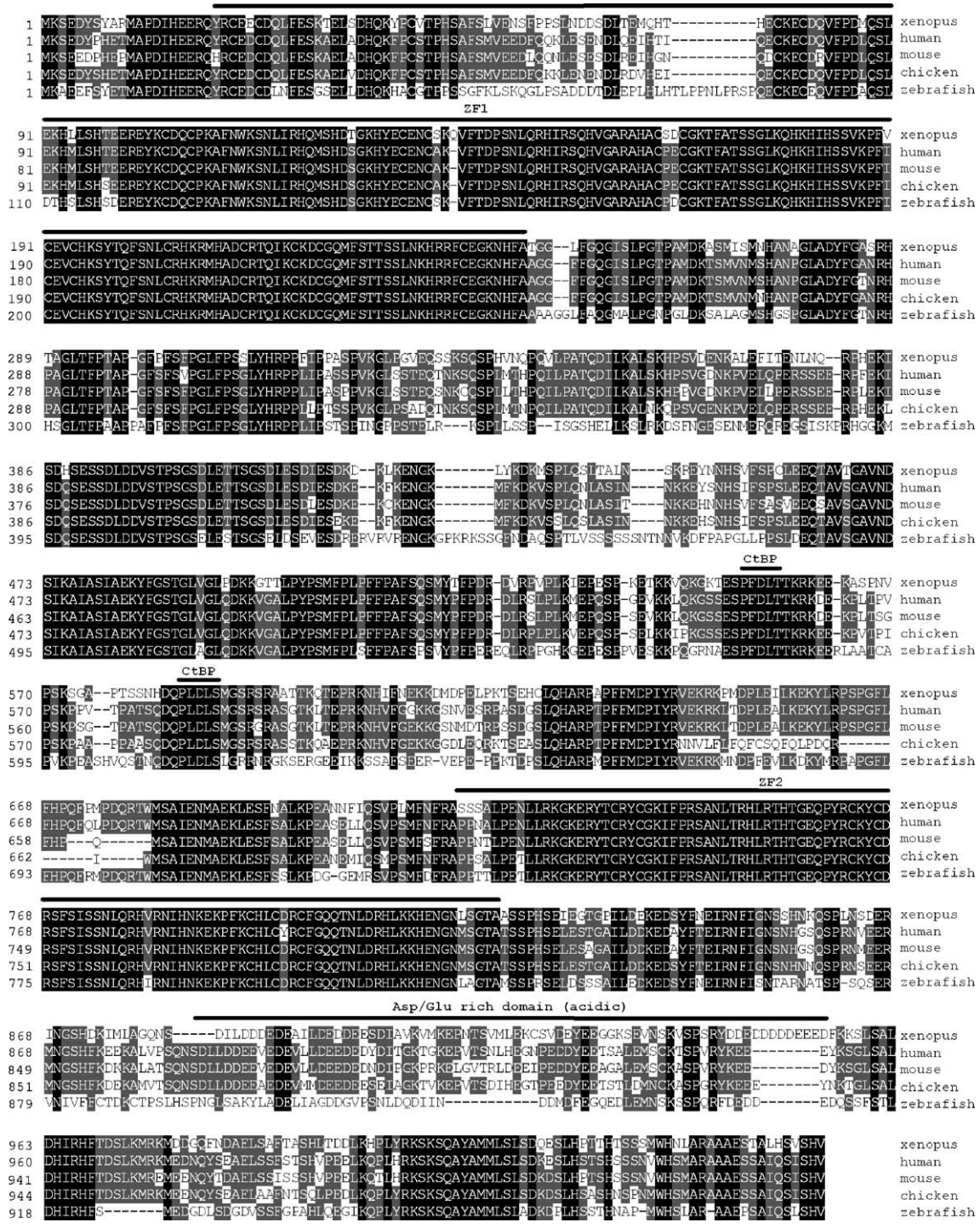

Fig. 1. Amino acid sequence alignment of *Xenopus* (*X.l*; DQ088677), human (*H.s*; CAA38735), mouse (*M.m*; NP 031989), predicted chicken (*G.g.*) and predicted zebrafish (*D.r.*) Evi1 proteins. The zinc fingers, CtBP binding sites and acidic regions are indicated.

Expression of Evi1 and related MEL1 genes

The *Evi1* expression pattern was analyzed in *Xenopus*, zebrafish and chick embryos. In *Xenopus* using RNAase protection assay, no maternal transcripts of *Evi1* could be detected. Zygotic expression begins at stage 20 and increases continuously until stage 40. In the adult, *Evi1* is expressed in various tissues including kidney, lung, testis, spleen and stomach (Fig. 2A). Consistent with the RNAase protection analysis, by whole-mount in situ hybridization, *Evi1* mRNA staining was first detected at stage 20 in the pronephric mesoderm (Fig. 2A, panel 1). Compared to *XPax8* expression which marks the entire presumptive pronephric region (Carroll and Vize, 1999), *Evi1* expression is restricted to the ventral posterior part of the pronephros anlagen (Fig. 2A, panel 4). Sections of stages 20–25 embryos confirmed this observation

and revealed that *Evi1* expression within the pronephric mesoderm is restricted to the somatic layer that gives rise to the pronephros anlagen. No expression is detected in the splanchnic layer that forms the glomus (Fig. 2A, panels 2, 5, 7). In the pronephros of early tadpole embryos, *Evi1* expression is, like that of *xClC-K* (Vize et al., 2003), restricted to the distal segment of the pronephric tubules and to the duct (Fig. 2A, panel 12). This expression in the pronephros persists at early tadpole stage (Fig. 2A, panels 15, 16) but is not detectable anymore at stage 40 (data not shown). In addition to expression in the developing pronephros, strong expression of *Evi1* is also detected from stage 21 in selected regions of the developing brain (Fig. 2A, panel 3). Analysis of stage 25 embryos reveals *Evi1* staining in the dorsal telencephalon, in the ventral diencephalon, in the midbrain and hindbrain (Fig. 2A, panels 6, 8). Double labeling with a *XKrox-20* probe that labels rhombomeres 3 and 5 (Bradley et al., 1993) shows that the initial *Evi1* expression domain in the hindbrain is found in rhombomere 4. In transverse sections of the hindbrain through r4, only the most dorsal part of the neural tube is labeled by the *Evi1* probe (Fig. 2A, panels 9, 10). In tadpoles, *Evi1* expression in the hindbrain expands anteriorly and posteriorly (Fig. 2A, compared panels 6 and 12). In transverse sections, transcription is also detected below the *Evi1* positive dorsal side of the neural tube in a subset of differentiated neurons (Fig. 2A, panel 13). Outside the brain, *Evi1* transcripts are found from late neurula stage in the olfactory placodes (Fig. 2A, panel 8) and in neural crest cells migrating towards the visceral arches. The strongest staining is observed in a population of crest cells that is found anteriorly to the *XKrox-20* expressing crest cells that migrate from r5 into the third arch (Bradley et al., 1993). These cells appear derived from r4 and thus correspond to the hyoid stream that migrates into the second visceral arch (Fig. 2A, panel 11). In tadpoles, strong *Evi1* expression is detected in the neural crest component of the arches and in head mesenchyme cells (Fig. 2A, panels 12, 14, 15).

A similar pattern of *Evi1* expression is seen in the zebrafish embryo. At the 2–4 somite stage, *Evi1* expression starts to be detected in the intermediate mesoderm and strong staining is detected in the telencephalon (Fig. 2B, panel 1). At the 8 somite stage, expression in the lateral plate becomes as prominent as in the forebrain and additional sites of expression appear in the head region (Fig. 2B, panels 2–4). The *Evi1* bilateral stripes of staining in the intermediate mesoderm extend less anteriorly than that of *Sim1*, considered as a pronephric duct specific transcription factor (Serluca and Fishman, 2001) (Fig. 2B panel 5). At the 17–20 somite stage, strong staining persists in the posterior part of the duct and additional staining was visualized in the anterior spinal cord, telencephalon, dorsal and ventral diencephalon, midbrain tegmentum, olfactory placodes, branchial arches and pectoral fins. In the hindbrain, *Evi1* transcripts are detected in one rhombomere, most probably rhombomere 4 (Fig. 2B, panels 6, 7). During the pharyngula stage, strong *Evi1* staining persists in the head. Expression of *Evi1* in the hindbrain which was initially restricted to a single rhombomere becomes increasingly complex and extends toward the posterior (Fig. 2B, panel 8).

In chicken embryos, *Evi1* expression is first observed at stages 8–9 in bilateral stripes in the intermediate mesoderm, extending from the 6th to the 11th somite (Fig. 2C, panel 1). At stage 11, strong *Evi1* expression persists in the nephric duct (Fig. 2C, panels 2, 3). In stage 19 embryos, *Evi1* expression in the duct has disappeared and strong staining is observed in the limb buds and branchial arches. Weak expression just above background may also be detected in the brain (Fig. 2C, panel 4).

Expression of *MEL1* was examined by in situ hybridization in *Xenopus* embryos. *MEL1* expression is first detectable at stage 23 in a single anterior streak of cells extending perpendicular to the neural tube that, based on its location with respect to the otic vesicle and on the similarity of the staining observed with the *Evi1* probe, appears to correspond to migrating hyoid crest cells (Fig. 2D, panel 1). At stage 24, *MEL1* starts to be expressed in all crest segments and transcripts are also detected in the otic vesicle and head mesenchyme (Fig. 2D, panel 2). At stage 28, strong *MEL1* expression is also detected in the most dorsal part of the hindbrain, in the retinal pigment epithelium, in the ventral part of the otic vesicle and in the midbrain and forebrain. In tadpoles, *MEL1* expression is also detected in the pronephric duct and distal tubule and in the heart (Fig. 2D, panels 3–8). Thus, *Evi1* expression profile is largely conserved in vertebrates and partially overlaps that of the related *MEL1* gene. Within the pronephros, *Evi1* and *MEL1* are sequentially selectively activated within the distal tubule and duct compartments, *Evi1* being expressed before any overt sign of pronephric morphogenesis.

The anterior and posterior portions of the zebrafish duct express distinct markers

The comparison of the *Evi1* expression patterns observed in *Xenopus* and zebrafish suggested to us that only the posterior part of the zebrafish duct might be equivalent to the distal tubule and duct compartments in *Xenopus*. To further test this hypothesis, we compared, in both species, the expression pattern of other genes known to be expressed in a restricted manner in the kidney. We first determined in zebrafish the expression of *ClC-K*, known in *Xenopus* to label the duct and distal tubule (Vize et al., 2003). We observed that *ClC-K*, like *Evi1*, labels only the posterior part of the duct (Figs. 3A, B). We, next, re-examined in zebrafish the expression of the *ret1* proto-oncogene (Marcos-Guterierrez et al., 1997) that labels in *Xenopus* only the duct (Osafune et al., 2002). Double staining with *Evi1* or *ClC-K* and *ret1* indicates that expression of both genes extends further anteriorly than that of *ret1*, which labels only the caudal-most portion of the duct (Figs. 3C–F). Based on those observations, we asked whether the anterior-most portion of the zebrafish duct, which is negative with distal tubule/duct markers, might express proximal tubule markers. Therefore we identified and analyzed the expression in zebrafish and *Xenopus* of the genes encoding the homologues of the mammalian anion transporter Sat1 (SLC26A1) and of the human multi–PDZ domain containing PDZK1 adaptator protein known to be specifically expressed in renal proximal tubular cells (Karniski et al., 1998; Kocher et al., 2003). We observed that in *Xenopus*,

as expected, both genes specifically mark the proximal tubules and that in zebrafish, they are only expressed in the anterior portion of the pronephric duct (Figs. 3G–J). Together, these observations indicate that although uniform in appearance, the zebrafish nephron is patterned along its A/P axis and that the anterior portion of the duct has functional properties characteristic of the *Xenopus* and mammalian proximal tubule compartment.

Evi1 expression in the pronephros is upregulated by retinoid signaling and repressed by overexpression of xWT1 and by Notch signaling

In *Xenopus*, there is evidence that, in addition to BMP, RA signaling might play an essential role in mesodermal patterning (Maden, 1999; Ruiz i Altaba and Jessell, 1991) and pronephros development (Taira et al., 1994; Blumberg et al., 1997;Chan et al., 2000; Osafune et al., 2002). As *Evi1* expression has been shown to be upregulated by retinoic acid treatment in cell culture (Aytekin et al., 2005; Kazama et al., 1999), we therefore set out to determine whether RA signaling might regulate *Evi1* expression in the context of the developing pronephros. Embryos that had been treated with 10 μM all-trans-RA during stages 9–10 show an enlargement of the *Evi1* expression domain (83% of the embryos, $n = 24$) (Figs. 4A, B). An increase of *Evi1* expression was also observed in embryos unilaterally injected with 2 ng of mRNA encoding XRALDH2, a major RA generating enzyme (Chen et al., 2001), and treated with 5 μM of its substrate, all-trans retinal (57% of the embryos, $n = 42$) (Figs. 4C, D). Blockage of RA signaling by injection of 2 ng of *xCYP26* mRNA which is a critical enzyme in RA degradation (Hollemann et al., 1998) resulted in a reduction of the expression of *Evi1* (79%, $n = 24$) on the injected side (Figs. 4E, F). Injection of embryos with 1 ng of mRNA encoding a dominant negative RARα receptor (xRARα1^{405*}) (Blumberg et al., 1997) caused a similar reduction of *Evi1* expression (53%, $n = 47$) (Figs. 4G, H). RA signals are thus required for *Evi1* expression in the developing *Xenopus* pronephros.

The restricted localization of *Evi1* within the distal tubule and duct compartments of the developing pronephros leads to the question of the mechanisms that regulate *Evi1* expression in this region. Notch signaling pathway has been shown to play an important role in the early selection of duct and tubule cell fates within the *Xenopus* pronephros anlagen (McLaughin et al., 2000). In mice, it has been shown to be required for proximal tubule and podocyte formation (Cheng et al., 2003; Wang et al., 2003; Cheng and Kopan, 2005). We therefore tested whether *Evi1* expression is regulated by Notch. Ligand activation of Notch results in the release of its cytoplasmic region (NICD) that can then translocate to the nucleus where it interacts with the transcriptional factor Suppressor of Hairless (Su(H)) to activate the expression of downstream target genes. To inhibit Notch activity, embryos were injected unilaterally at the 8-cell stage into the lateral marginal zone with 500 pg of mRNA

Fig. 2. Embryonic expression pattern of *Evi1* and *MEL1*. (A) *Evi1* in *Xenopus*. Top panels: RNAase protection analysis of *Evi1* transcripts during oogenesis and embryogenesis (left) and in adult organs (right). *FGFR* or *EF1α* are used as internal controls. Bottom panels: whole-mount in situ hybridization analysis of *Evi1* expression. Embryos were fixed at the indicated Nieuwkoop-Faber stages and analyzed with the probes as indicated. (1–5) Expression of *Evi1* at late neurula stage. (1) Initial expression of *Evi1* is observed in the pronephric mesoderm. (2) Transversal section of the embryo shown in (1) showing restricted *Evi1* expression in the somatic layer. (3) Dorsal view of a slightly later stage embryo showing *Evi1* expression in selected regions of the developing brain. (4) Comparison of *Evi1* (purple) and *Pax8* (light blue) expression in the pronephros; note that *Evi1* expression is restricted to the ventral posterior part of the *Pax8* expression domain. (5) Transversal section at the level of the pronephros. (6–11) *Evi1* expression at tailbud stages. (6) Lateral view of an embryo; note *Evi1* expression outside the pronephros in the forebrain, midbrain and hindbrain and in cranial neural crest cells. (7) Transversal section of the embryo shown in (6) at the level indicated; note that *Evi1* expression can be seen only in the ventral part of the pronephros anlagen. (8) Horizontal section showing *Evi1* expression in the dorsal telencephalon, ventral diencephalons and in the olfactory placodes. (9) Transversal section at the level of r4 in the hindbrain; note that only the dorsal part of the neural tube is labeled by the *Evi1* probe. (10) High-magnification view of the hindbrain with anterior towards the top double stained with *Evi1* (red) and *XKrox20* (purple) probes indicating that *Evi1* is expressed in r4. (11) Embryo double stained with *Evi1* (light blue) and *XKrox-20* (purple); note that the *Evi1* strongest staining in the migrating neural crest cells is found anteriorly to the *XKrox-20* expressing cells. (12–16) *Evi1* expression at tadpole stages. (12) High-magnification view of the head; note that *Evi1* expression is restricted to the posterior part of the pronephros and that in the hindbrain, its expression initially restricted to r4 has expanded anteriorly and posteriorly. (13) Transversal section at the level of the otic vesicles; note that *Evi1* expression can be seen in addition to the dorsal neural tube in a subset of differentiated neurons. (14) Horizontal section through the visceral arches, with anterior towards the right; note *Evi1* expression in the neural crest component of the branchial arches. (15) Lateral view of a late tadpole; note that within the pronephros, *Evi1* expression is restricted to the distal tubule and duct compartments. (16) Transversal section at the level of the trunk showing *Evi1* expressing pronephric duct cells. (B) Whole-mount in situ analysis of *Evi1* expression in zebrafish. (1) In 4S stage embryos, strong *Evi1* staining is apparent in the telencephalon. (2, 4) Lateral view, dorsal view and transversal section of a 8S stage embryo; note additional *Evi1* staining in the intermediate mesoderm and in the head region. (5) Dorsal view of an embryo stained with a *Sim1* probe; note that *Sim1* expression in the intermediate mesoderm extends further anteriorly than Evi1. (6, 7) Lateral and dorsal view of stages 17S–20S embryos. Note that *Evi1* is expressed in various regions of the brain, in head neural crest cells and in the posterior part of the pronephric duct. (8) Lateral view of a pharyngula stage embryo; note that *Evi1* expression in the hindbrain has extended posteriorly and that it is also strongly expressed in the pectoral fins. (C) Whole-mount in situ analysis of *Evi1* in chick. (1) Dorsal view of a stage 9 embryo showing *Evi1* expression in the intermediate mesoderm. (2, 3) Dorsal view and transversal section of a stage 11 embryo showing *Evi1* expression in the nephric duct. (4) In 19S embryos, *Evi1* expression in the duct has disappeared and strong staining is detected in the limb buds. (D) Whole-mount in situ analysis of *MEL1* in *Xenopus*. (1, 2) Lateral views of early tailbud stage embryos. Note *MEL1* expression in cranial crest cells, in the head mesenchyme and in the otic vesicle. (3, 5) High magnification view of the head and transversal sections of early tadpoles. Note that *MEL1* staining is now also apparent in various parts of the brain and in the retinal pigment epithelium. (6–8) Lateral view and horizontal sections of late tadpoles. Note that additional *MEL1* staining is seen in the heart and in the pronephric distal tubule and duct. Abbreviations: a1–a4, arch 1–4; ba, branchial arches; bcs, branchial crest segment; cnc, cranial neural crest; dd, dorsal diencephalon; dt, dorsal telencephalon; e, eye; fb, forebrain; hb, hindbrain; hcs, hyoid crest segment; h, heart; hm, head mesenchyme; im, intermediate mesoderm; lb, limb buds; mcs, mandibular crest segment; mb, midbrain; nc, notochord; nd, nephric duct; nt, neural tube; olp, olfactory placodes; ov, otic vesicle; pf, pectoral fins; pn, pronephros; pnd, pronephric duct; pndt, pronephric distal tubule; ppnd, posterior pronephric duct; rpe, retinal pigment epithelium; r3–5, rhombomere 3–5; sc, spinal cord; som, somatic lateral plate mesoderm; spm, splanchnic lateral plate mesoderm; tel, telencephalon; tg, tegmentum; va, visceral arches; vd, ventral diencephalon.

encoding a dominant negative form of Su(H), (Su(H)DBM). To activate Notch signaling, embryos were injected with 500 pg of mRNA encoding the activated form of Notch, NICD (Coffman et al., 1993; Wettstein et al., 1997). Figs. 4I, J show that substantial increase in the expression of *Evi1* was detected in embryos injected with the *Su(H)DBM* construct (83%, $n = 34$). In contrast, embryos injected with 500 pg of *NICD* mRNA show a reduction of *Evi1* (95%, $n = 47$) on the injected side (Figs. 4K, L). A similar reduction was observed upon injection of mRNA encoding inducible downstream effectors of the Notch pathway such as *XHRT1* which is expressed in the dorso-anterior portion of the pronephros anlagen (V. Taelman, unpublished observations). We conclude that Notch signaling represses *Evi1* expression and is thus required in *Xenopus* like in the mouse for the early selection of proximal tubule versus distal tubule and duct cell fates.

Transcription factors that are involved in the regionalization of the pronephric mesoderm are not well known. Previous studies have shown that the *xWT1* gene is expressed in the pronephric splanchnic mesoderm giving rise to the glomus and that it may play a role in the restriction of the expression of early pronephric markers such as *Xlim-1* and later tubule specific markers to the somatic layer (Carroll and Vize, 1996; Wallingford et al., 1998). Therefore we asked whether xWT1 also negatively regulates *Evi1* expression. Injection of 250 pg *xWT1* mRNA into one side of the lateral marginal zone of 8-cell stage embryos suppressed *Evi1* expression on the injected side (82%, $n = 51$) (Figs. 4M, N). Altogether, these results indicate that RA signaling is required for *Evi1* expression in the developing pronephros and that activation of Notch signaling in the dorso-anterior part of the pronephros and *xWT1* contributes to its restricted expression in the ventral–posterior portion of the pronephric primordium.

Evi1 overexpression from late neurula stage specifically inhibits the expression of proximal tubule and glomus pronephric markers

To evaluate *Evi1* function in pronephros formation, we overexpressed it in the embryo. Eight cell stage were injected into one blastomere in the lateral marginal zone with 500 pg of *Evi1* mRNA. Injected embryos developed normally until the

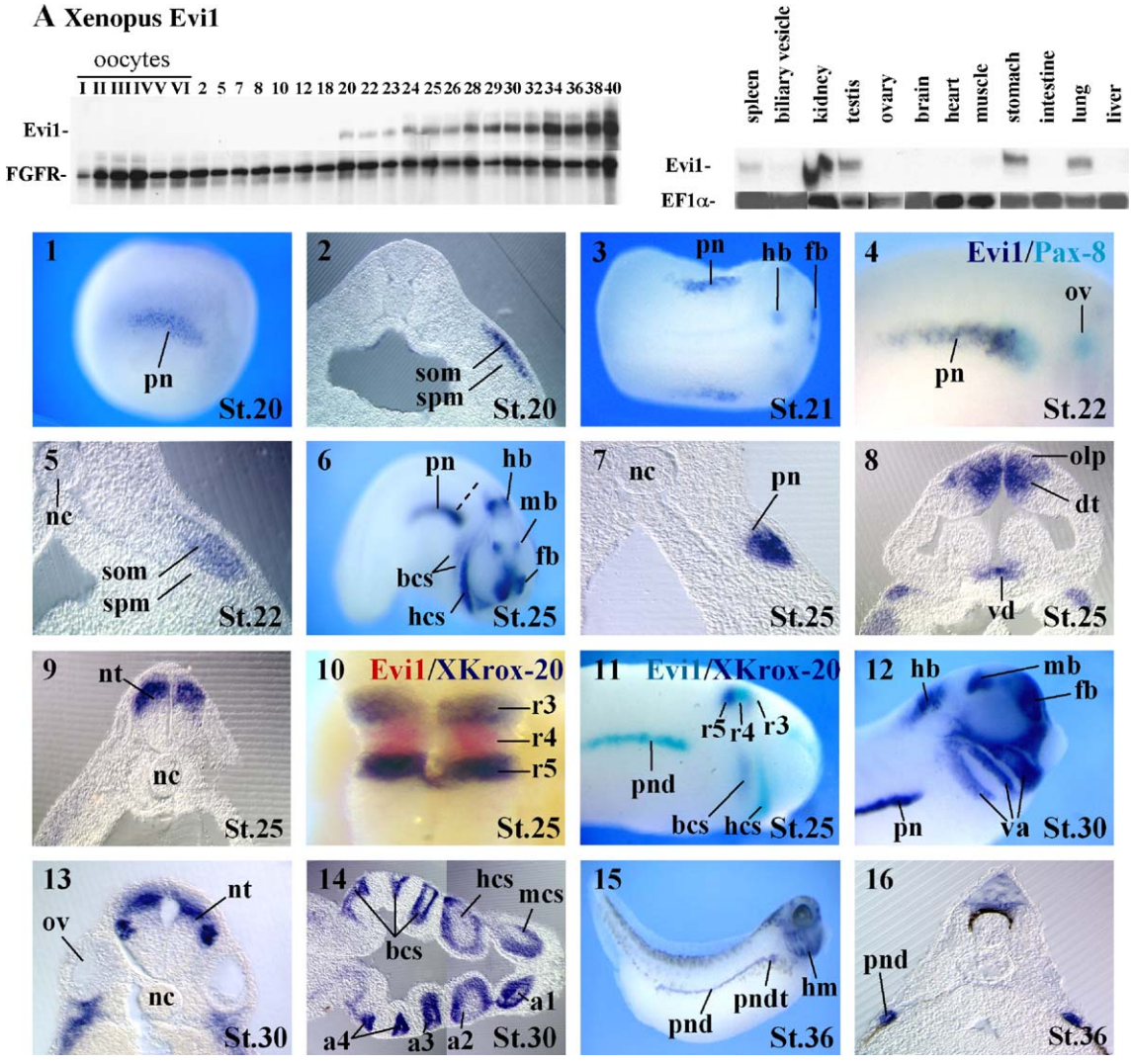

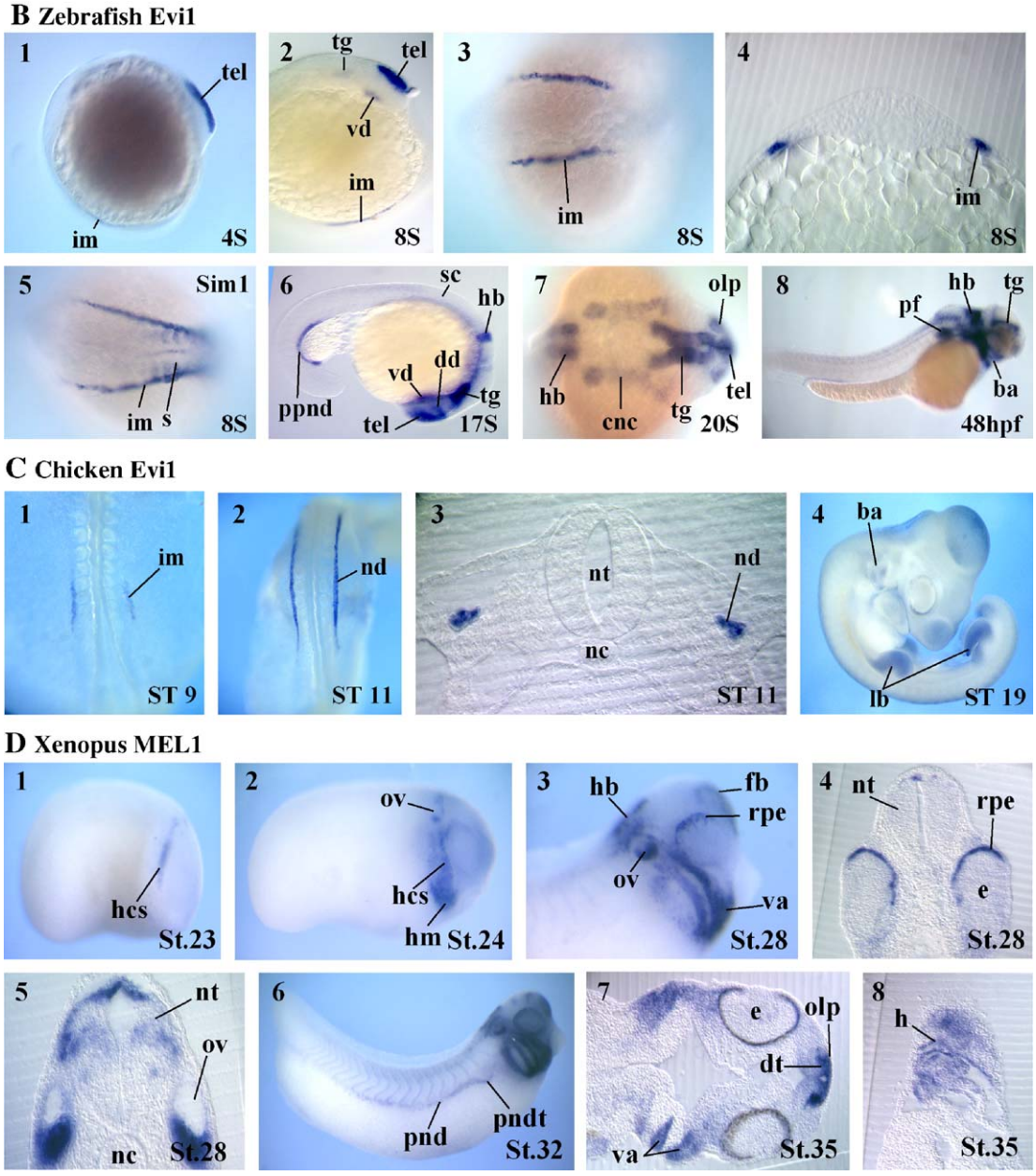

Fig. 2 (*continued*).

gastrula stage but then failed to complete gastrulation (Fig. 5A). Whole-mount in situ analysis revealed that *Evi1* overexpression resulted in a dramatic repression of the expression of mesodermal markers such as the transcription factor *brachyury* (*Xbra*) (100%, n = 43 embryos) and the secreted polypeptide *chordin* (100%, n = 18 embryos) (Figs. 5B, C). In contrast, at identical concentration, *Evi1* microinjection in the animal pole did not affect the expression of the ectodermal marker *epidermal keratin* (none repressed, n = 27), the early neural crest marker *Slug* (none repressed, n = 17) and the pan-neural *Sox2* marker (none repressed, n = 22) (Figs. 5D–F). Evi1 has been shown to repress TGF-β signaling by binding to Smad3 through the first finger domain (Kurokawa et al., 1998). Interestingly, we observed that overexpression of a construct encoding the N-terminal part of the Evi1 protein including the entire first zinc finger domain and non-finger central region repressed the expression of *chordin* as efficiently as the wild type protein. In contrast, a construct encoding the C-terminal portion of the Evi1 protein consisting of the second zinc finger domain and downstream sequences was much less active (data not shown). The unspecific phenotype we observed in early embryos upon overexpression of Evi1 might thus occur through repression of TGF-β signaling.

In order to overcome the early effects of *Evi1* on mesoderm development, we generated an inducible Evi1 construct by fusing the entire coding region of *Evi1* to the ligand-binding domain of the human glucocorticoid receptor (hGR) (Gammill and Sive, 1997). Embryos at the 8-cell stage were injected into one blastomere in the lateral marginal zone with 250 pg of *Evi1-hGR* mRNA. Addition of dexamethasone at blastula stage

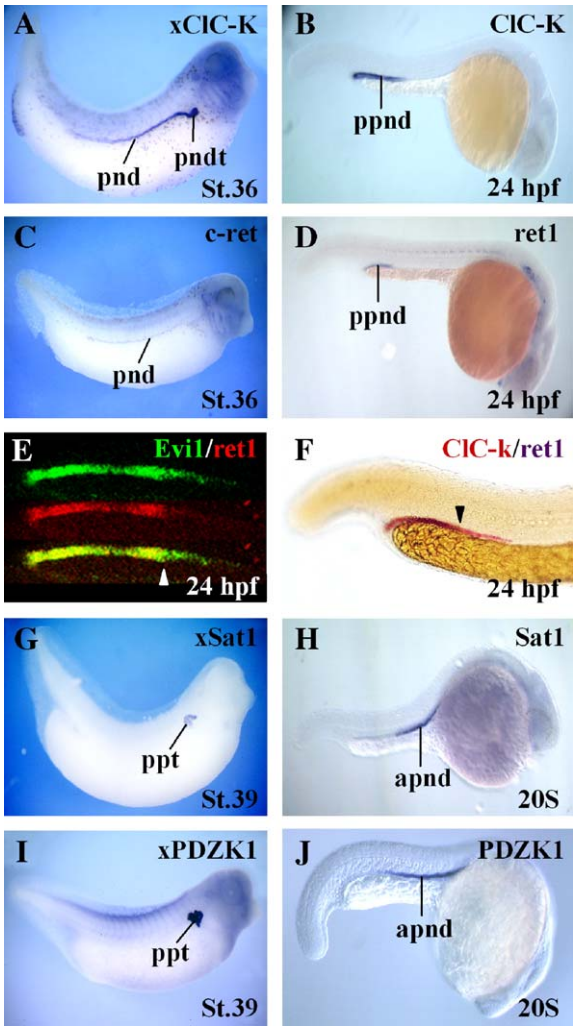

Fig. 3. Comparison of *ClC-K*, *ret*, *Sat1*, *Evi1* and *PDZK1* expression in *Xenopus* and zebrafish pronephros. The stages and probes analyzed are indicated in each figure. Anterior is toward the right. (A–D,G–J) Single in situ hybridization of the indicated markers. Note that in zebrafish *ClC-K* and *ret1* expression is restricted to the posterior part of the duct while the proximal tubule specific markers *Sat1* and *PDZK1* are expressed in its anterior portion. (E) Comparison by fluorescent in situ hybridization of *Evi1* (green) and *ret1* (red) expression in a 24-hpf zebrafish embryo. Note that *Evi1* expression extends further anteriorly than that of *ret1*. (F) Comparison by double in situ hybridization of *ClC-K* (red) and *ret1* (purple) expression in a 24-hpf zebrafish embryo. Note that *ClC-K* expression extends further anteriorly than that of ret1. Abbreviations: apnd, anterior pronephric duct; pnd, pronephric duct; pndt, pronephric distal tubule; ppnd, posterior pronephric duct; ppt, proximal pronephric tubules.

(stage 8) caused a hormone dependent loss of expression of *Xbra* at stage 10.5 (data not shown), which is consistent with the phenotype observed in embryos injected with *Evi1* mRNA (Fig. 5) and suggests that this fusion construct is fully active. Dexamethasone treatment at the neurula stage (+Dex stage 18) resulted in a hormone dependent manner in the reduction at tadpole stage of the expression of all proximal tubule specific markers tested, including early one such as *X-Delta-1* (68% inhibited, $n = 21$) and *EphA4* (52% inhibited, $n = 28$) and later markers such as *xSat1* (67% inhibited, $n = 49$) and *XSMP-30* (58% inhibited, $n = 61$) (Chitnis et al., 1995; Smith et al., 1997; Sato et al., 2000) (Figs. 6A–H and data not shown). Overproduction of Evi1 at the neurula stage also produced an inhibition at tailbud stage of the expression of the *xWT1* (Carroll and Vize, 1996) and *nephrin* (Gerth et al., 2005) glomus markers (71% and 57% inhibited, $n = 23$ and 17 respectively) (Figs. 6K–R). In those injected embryos, the pronephric anlagen and the splanchnic layer appear, however, at tailbud stage visible and of normal size (Figs. 6M, N, Q, R). In contrast, at the same dose, no such inhibitory effect was observed at such frequency on markers that label the distal tubule and/or duct such as *GATA-3* (Deconinck et al., 2000) (15% inhibited, $n = 23$), *Gremlin* (12% inhibited, $n = 24$) (Hsu et al., 1998) and *xClC-K* (13% inhibited, $n = 44$) (Figs. 6G–J and data not shown). We did not observe changes in *Pax-8* and *Xlim-1* (Carroll and Vize, 1999; Chan et al., 2000) expression either in *Evi1-hGR* mRNA injected embryos, which is consistent with Evi1 functioning downstream of those early pronephric specification genes (data not shown). Thus, the effects of *Evi1-hGR* on pronephric markers appear specific.

The first zinc finger and CtBP interaction domains are required for Evi1 activity in the pronephros

Evi1 has been shown to encode a transcriptional repressor. Two regions of *Evi1* are required for its full repression activity. One of these regions is the first zinc finger domain that interacts with Smad3 and the second one is a repressor domain located upstream of the second zinc finger domain that has CtBP binding sites (Kurokawa et al., 1998; Palmer et al., 2001). We found that *Xenopus* Evi1, like murine and human Evi1 proteins, interacts with CtBP (data not shown). To determine the importance of those two domains for Evi1 activity in the pronephros, we generated three Evi1 deletion mutants, Evi1ΔZF1-hGR, Evi1ΔZF2-hGR and Evi1ΔCtBP-hGR and tested as above their ability to repress *XSMP-30* expression when activated in the pronephric mesoderm at neurula stage. While Evi1ΔZF2-hGR was as effective as the wild type protein (52% inhibited, $n = 63$), Evi1ΔZF1-hGR and Evi1ΔCtBP-hGR had no effect on *XSMP-30* expression (none inhibited, $n = 93$ for Evi1ΔZF1-hGR and $n = 71$ for Evi1ΔCtBP-hGR) (Fig. 7). These results indicate that both the ZF1 domain and the CtBP binding sites are important for Evi1 activity. Evi1 thus functions in the pronephros as a CtBP dependent repressor.

Injection of Evi1-VP16-hGR mRNA with activation at neurula stage disrupts distal tubule and duct formation and expands glomus and early proximal tubules markers

Based on our results suggesting that *Evi1* functions as a repressor in the pronephros, to interfere with this function, we generated an inducible mutant, *Evi1-VP16-hGR*, in which the entire *Evi1* sequence is fused to the strong activation domain of VP16. We anticipated that this chimera would interfere with the activity of the wild type protein. Consistent with this prediction, injection of 500 pg *Evi1-VP16-hGR* mRNA into

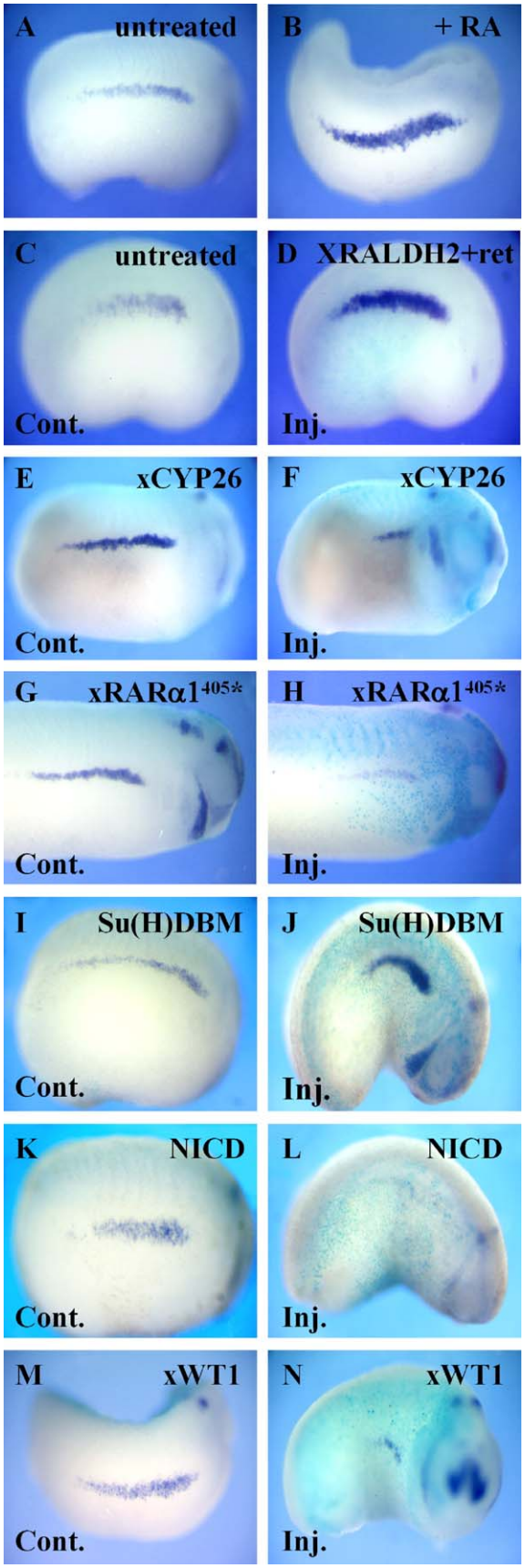

one blastomere of the lateral marginal zone of 8-cell stage embryos with addition of DEX from neurula stage (stage 18) caused opposite effects to native Evi1. Evi1-VP16-hGR disrupted the formation of the distal tubule and duct, as visualized morphologically in tadpole embryos and following the expression of *GATA-3*, *Gremlin* and *xClC-K* markers (71%, 78% and 65% inhibited, n = 17, 26 and 29, respectively) (Figs. 8A–D and data not shown) and caused the expression of *xWT1* and *nephrin* to increase and to expand ventrally and posteriorly within the splanchnic layer (76% and 53%, n = 37 and 21, respectively) (Figs. 8E–J). Injection of mRNA encoding VP16 alone had no such effects (data not shown). Injection of *Evi1-VP16-hGR* mRNA also resulted, at tailbud stages, in some embryos in a ventral–posterior expansion within the pronephros anlagen of the expression of *X-Delta-1* and *EphA4* which are normally restricted to its dorso-anterior portion (21% and 26%, n = 53 and 19, respectively) (Figs. 8K–P). At tadpole stages, a decrease in the expression of proximal-tubule specific markers such as *xPDZK1*, *XSMP-30* and *xSat1* was however observed in most injected embryos (68%, 74% and 65%, n = 21, 38, and 26, respectively) (Fig. 8Q and data not shown). Interestingly, an expansion of the expression of the proximal tubule markers and small ectopic positive cells within a more posterior region of the intermediate mesoderm could be observed in a few cases (15%, n = 37) (Figs. 8R–T). Such ectopic proximal tubule-positive cells were never observed in *Evi1-hGR* mRNA injected embryos.

To further determine the role of *Evi1*, we attempted a knockdown of *Evi1* function using morpholino antisense oligonucleotides in *Xenopus laevis*. We designed two morpholinos targeting the 5′ end of the mRNA close to the AUG initiation codon that specifically blocked translation of *Evi1*, both in a reticulocyte translation system and in vivo. Injection of those Evi1 inhibitory morpholinos did not inhibit development of the distal tubule and duct. As this lack of phenotype may be due to the other Evi1 pseudoallele not yet identified, we repeated those initial morpholino experiments in *Xenopus tropicalis*. In vitro and in vivo, the designed morpholino efficiently blocked translation of its target. However, as in *Xenopus laevis*, we were unable to observe a phenotype in the depleted embryos (data not shown). Although the absence of Evi1 appears not sufficient to perturb duct and distal tubule formation, these results are consistent with the overexpression

Fig. 4. *Evi1* expression in the pronephros is upregulated by retinoid signaling and repressed by *xWT1* and Notch signaling. Embryos were injected with the indicated mRNA together with β-*galactosidase* mRNA and processed at tailbud stage by whole-mount in situ hybridization to visualize *Evi1* expression. In all panels, anterior is to the right. Control and injected sides revealed with X-gal are shown. (A–H) *Evi1* expression is elevated in embryos by RA treatment or by injection of mRNA encoding XRALDH2 in the presence of its substrate, all-trans retinal. Conversely, it is decreased in embryos where RA signaling is inhibited by injection of *xCYP26* mRNA or the dominant negative *RARα receptor xRARα1*^{405*}. (I–L) *Evi1* expression is increased in embryos where Notch signaling is inhibited by injection of mRNA encoding the dominant negative form of Su(H), Su(H)DBM. Conversely, a reduction of *Evi1* expression is observed in embryos overexpressing the activated form of Notch, NICD. (M, N) *Evi1* expression is downregulated by *xWT1* mRNA injection.

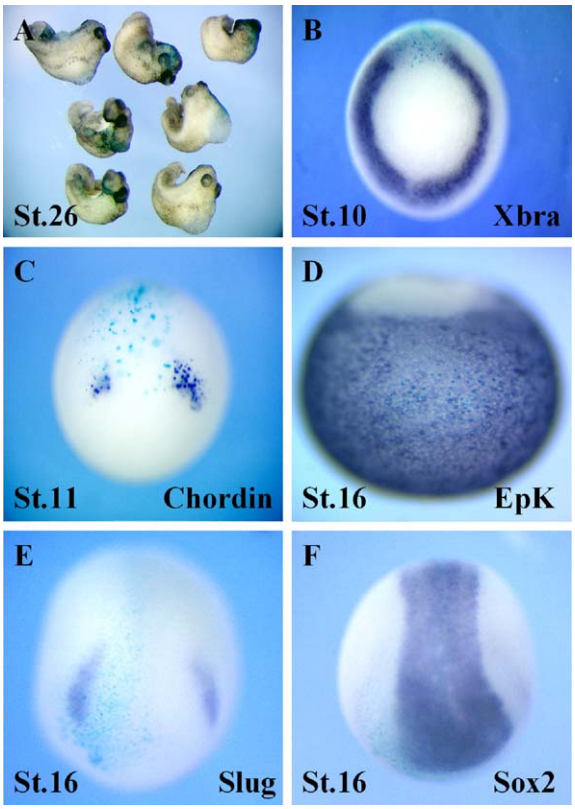

Fig. 5. Overexpression of *Evi1* down-regulates *Xbra* and *chordin* expression but not other genes in the early *Xenopus* embryo. (A) Embryos injected with *Evi1* mRNA failed to complete gastrulation. (B–F) Whole-mount in situ analysis of the indicated markers in embryos coinjected with *Evi1* and *β-galactosidase* mRNA. In all cases, β-galactosidase activity is revealed with X-gal. (B, C) Vegetal views of injected embryos at early gastrula stage. A reduction of the expression of the mesodermal markers *Xbra* and *chordin* is seen in the injected area. (D–F) Anterior view (D) and dorsal views (E, F) of neurula stage injected embryos analyzed for the expression of the ectodermal *EpK*, the neural crest *Slug* and the neural *Sox2* marker. Note that *Evi1* mRNA injection has no effect on the expression of these markers.

data and further suggest that Evi1 plays a role in the regionalization of the pronephros.

Discussion

In this study, we show that in *Xenopus* and zebrafish, *Evi1* and *MEL1* expression are detected sequentially in the posterior region of the developing pronephros that corresponds to the distal tubule and duct. Likewise in chicken, *Evi1* is also selectively expressed starting from stage 8 in the developing nephric duct. *Evi1* expression in the pronephros anlagen requires RA signals and is down-regulated by Notch and the zinc finger transcription factor xWT1, which are major players in the regionalization of the pronephros. *Evi1* overexpression at late neurula stage, using a hormone-inducible construct, specifically blocks proximal tubule and glomus formation. Conversely, overexpression of an inducible antimorphic Evi1-VP16 construct inhibits distal tubule and duct formation, expands the expression of glomus markers and can also induce ectopic proximal tubules. These results indicate that *Evi1* plays a role early in nephrogenesis.

Expression and regulation of Evi1

In the *Xenopus* and zebrafish pronephros, we found that *Evi1* expression is very similar to that of *ClC-K* and is thus restricted to the duct and distal portion of the tubules. In the developing urinary system of the mouse, *Evi1* has been reported to be expressed in the mesonephric duct and tubules and in metanephric tubules (Perkins et al., 1991). It will be interesting to get more information about the precise localization of *Evi1* along the mouse nephron to determine whether its expression in mammalian tubules is, like in *Xenopus*, restricted to the distal segment.

In the zebrafish pronephros, we found that the *Evi1* expression as well as that of *ClC-K* is restricted to the posterior portion of the duct and that their rostral limit of expression extends less anteriorly than that of the *Sim1* gene, a marker of the duct (Serluca and Fishman, 2001). Conversely, the anterior pronephric duct expresses a number of genes, including *Sat1* and *PDZK1* that both in *Xenopus* and in mammalian are expressed specifically in the proximal tubules segment (Fig. 3) (Karniski et al., 1998; Kocher et al., 2003). Our results thus indicate that the *Sim1* gene is not functionally a specific marker of the duct compartment. They also support the idea that in zebrafish the anterior segment of the duct is not duct at all but corresponds to proximal tubules. We also observed that the anterior limit of *Evi1*/*ClC-K* expression in the zebrafish pronephric nephron extends further anteriorly than that of *ret1*, a duct specific marker (Marcos-Gutiérrez et al., 1997; Osafune et al., 2002), suggesting that only the most distal portion of the zebrafish nephron is equivalent to the duct subdivision in *Xenopus* pronephric and mammalian metanephric kidney and that the portion of the nephron that expresses *Evi1*/*ClC-K* but not *ret1* may have characteristics of the distal tubule segment. The compartmentalization of the zebrafish nephron appears thus globally similar to that of *Xenopus* and mammalian.

We found that activation of RA signaling enhances, whereas inhibition of RA signaling inhibits, *Evi1* expression. This result is in accordance with the recent observation that the expression of specific *Evi1* mRNAs variants is increased by RA (Aytekin et al., 2005). As there is evidence that RA also affects the expression of the *Xlim-1* gene, which constitutes one of the earliest pronephric markers (Blumberg et al., 1997; Taira et al., 1994; Chan et al., 2000), RA might play an essential role in pronephric mesoderm specification. This idea is also supported by the observation that the genes encoding the synthetizing and catabolizing enzymes XRALDH2 and XCYP26 are expressed in the mesoderm during gastrulation (Hollemann et al., 1998; Chen et al., 2001). Further experiments are required to test this hypothesis and to define the direct targets of this pathway. In addition to the pronephros, *Evi1* is also strongly expressed in rhombomere 4 of the hindbrain. It will be of interest to test whether *Evi1* expression in the hindbrain is also controlled by RA and whether its expression is related to that of other genes encoding transcription factors involved in hindbrain segmentation and known to respond to RA such as *vhnf1* (Hernandez et al., 2004).

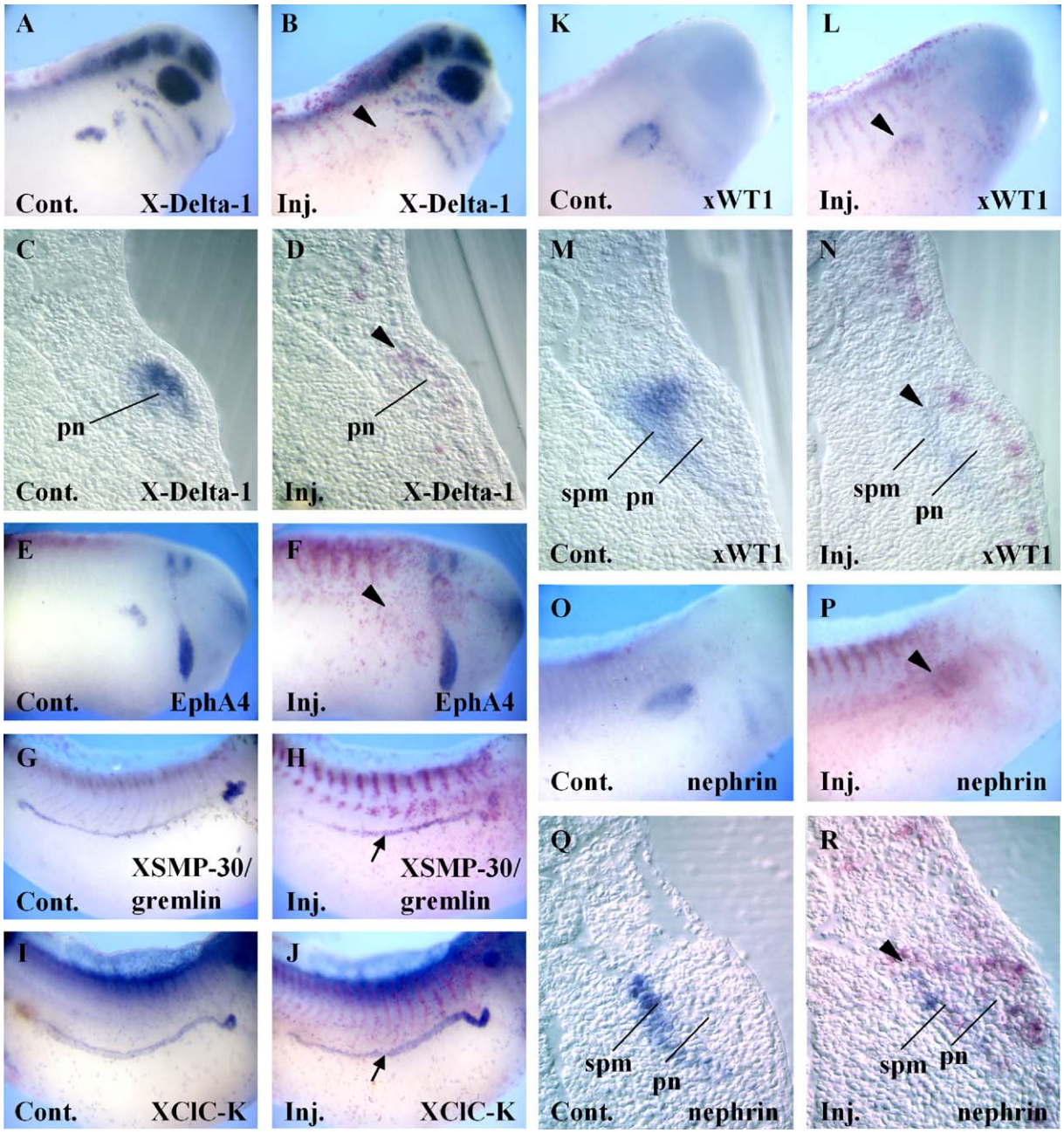

Fig. 6. Overexpression of *Evi1-hGR* in the pronephros with DEX addition from stage 18 specifically suppresses the expression of proximal but not distal markers. (A, B, E–L, O–P) Lateral views and (C, D, M, N and Q, R) sections through the pronephros of tailbud or early tadpole stage embryos coinjected with *Evi1-hGR* mRNA and *β-galactosidase* mRNA and stained with the indicated markers. Control and injected sides marked with Red-gal are shown. Note the reduction of the expression of the *X-Delta-1* (A–D), *EphA4* (E,F) and *XSMP-30* (G, H) proximal tubule and *xWT1* (K–N) and *nephrin* (O, R) glomus markers (arrowheads) while the expression of the *Gremlin* (G, H) and *xClC-K* (I, J) distal tubule and duct markers is unaffected (arrow). Abbreviations: pn, pronephros; spm, splanchnic layer of the mesoderm.

The Notch pathway has been shown to be required for proximal tubule and podocyte formation (Cheng and Kopan, 2005; Cheng et al., 2003; Wang et al., 2003). In *Xenopus*, it has been shown to favour proximal tubule formation at the expense of the duct (McLaughin et al., 2000). In this study, we showed that *Evi1* is strongly expressed at early tailbud stage in the ventro-posterior portion of the pronephric anlagen and that its activation correlates with that of *X-Delta-1* in the dorso-anterior part of the pronephros. Activation of Notch reduces, whereas blocking of Notch signaling expands *Evi1* expression in the pronephros. These results indicate that *Evi1* is regulated by Notch and that, like in the mouse Notch, controls the early selection of proximal tubule versus distal tubule and duct cell fates. Further experiments are required to identify the specific ligands and downstream effectors of the Notch pathway that are involved in pronephros development.

We found that misexpression of the *xWT1* zinc finger gene, which is normally selectively expressed in the splanchnic layer, also prevented *Evi1* expression. *Evi1* expression may thus be restricted to the ventro-posterior portion of the pronephros

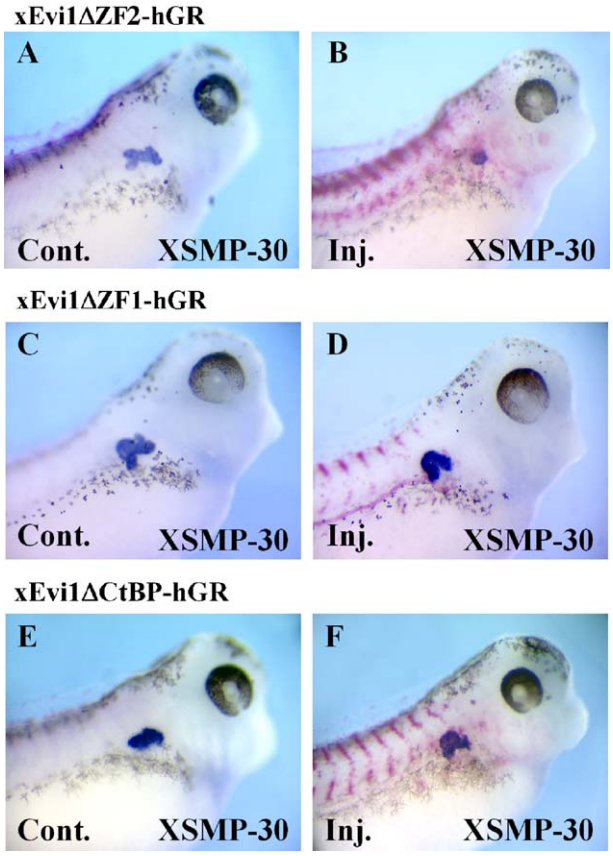

Fig. 7. Test of Evi1 ZF1, ZF2 and CtBP mutants for their ability to inhibit *XSMP-30* expression. Embryos overexpressing the indicated inducible Evi1 mutants were fixed at tadpole stage (stage 36) and the expression of the *XSMP-30* proximal tubule marker was analyzed. Control and injected sides marked with Red-gal are shown. Note that while Evi1ΔZF2-hGR is as effective as the wild type protein to repress *XSMP-30* expression (A, B), the deletion of ZF1 or the CtBP interaction motifs abolishes Evi1 activity (C–F).

anlagen due to the combined negative effects of Notch and xWT1. Further studies will be needed to understand the interactions between those two regulators.

Outside the pronephros, as in the mouse (Hoyt et al., 1997; Perkins et al., 1991; Morishita et al., 1990) *Evi1* is strongly expressed in specific areas of the brain, in the visceral arches and, in zebrafish and chicken, in limb buds. This strong overall similarity of the expression pattern of *Evi1* in vertebrates suggests that it plays an important conserved role throughout vertebrate evolution. One exception concerns the expression in the ovary. Morishita et al. (1990) showed that murine *Evi1* is actively transcribed in developing oocytes. However, in our RNAase protection assays, we did not observe *Evi1* expression during oogenesis, at least at a level comparable to that detected in the embryos.

Function of Evi1 in pronephros development

In addition to its role in the normal development of haematopoietic cells and leukaemia (Buonamici et al., 2004; Yuasa et al., 2005), Evi1 also appears to play an important role in a variety of other cell types. Indeed, mice lacking *Evi1* exhibit widespread hypocellularity, haemorrhaging and a disruption of the development of paraxial mesenchyme and, as a result, die at around 10.5 days post coitum (Hoyt et al., 1997). To analyze the role of Evi1 in pronephros development, we have generated hormone inducible overexpressing and inhibitory constructs. We show that misexpression of *Evi1* (*Evi1-hGR*) at the end of neurulation specifically inhibits proximal tubule and glomus formation. In contrast, misexpression of the *Evi1-VP16-hGR* interfering mutant disrupts distal tubule and duct formation and expands the expression of glomus markers. Expression of early proximal tubule markers such as *X-Delta-1* or *EphA4* in the pronephros is expanded ventrally. While tubule inhibition is observed in many Evi1-VP16-hGR embryos, in a few cases, ectopic proximal tubule positive cells were observed. We do not know the basis of this variability. The expansion of *xWT1* expression, which sometimes results in decreased size of the pronephros anlagen, may play a role in this phenomenon. Based on these observations, we propose that one early role of *Evi1* is to contribute together with other factors such as *XPax2* (Majumdar et al., 2000) to the restriction of the expression domain of *xWT1* to the splanchnic layer of the mesoderm. Another early role of *Evi1* expression would be to subdivide the pronephros anlagen into presumptive proximal tubule versus distal tubule and duct. In this hypothesis, Notch favors proximal tubule and inhibits distal tubule and duct cell fates by repressing *Evi1* gene expression in the dorso-anterior part of the pronephros anlagen.

Although our data indicate that *Evi1* expression plays a role in the early patterning of the pronephros, its importance in the differentiation of the distal tubule and duct is still not clear. Indeed, in contrast to the phenotype observed upon overexpression of *Evi1-VP16*, blocking Evi1 function with antisense morpholino oligonucleotides did not result in any clear phenotype. In accordance with this observation, in *Evi1* mutant mice, the mesonephric duct is small and hypocellular but clearly visible at day 10.5 (Hoyt et al., 1997). As in this mutant, the full-length and not an alternately transcript was disrupted, further investigation is required to establish the importance of Evi1 in mammalian nephrogenesis. One possible explanation for this lack of phenotype is that its absence may be compensated by the presence of another related factor. One obvious candidate is the related MEL1 transcription factor that although activated later than Evi1, is also selectively expressed in the pronephros in the distal tubule and duct compartments. Recent studies have shown indeed that MEL1 has similar DNA-binding activity and the same transforming capability for haematopoietic cells as *Evi1* (Mochizuki et al., 2000; Nishikata et al., 2003). This hypothesis remains to be experimentally tested.

Evi1 mechanisms of action

Evi1 is a complex two-handed zinc finger protein that is able to function both as transcriptional activator and repressor (Delwel et al., 1993; Morishita et al., 1995; Hirai, 1999; Nishikata et al., 2003). Our results demonstrate that an Evi1-

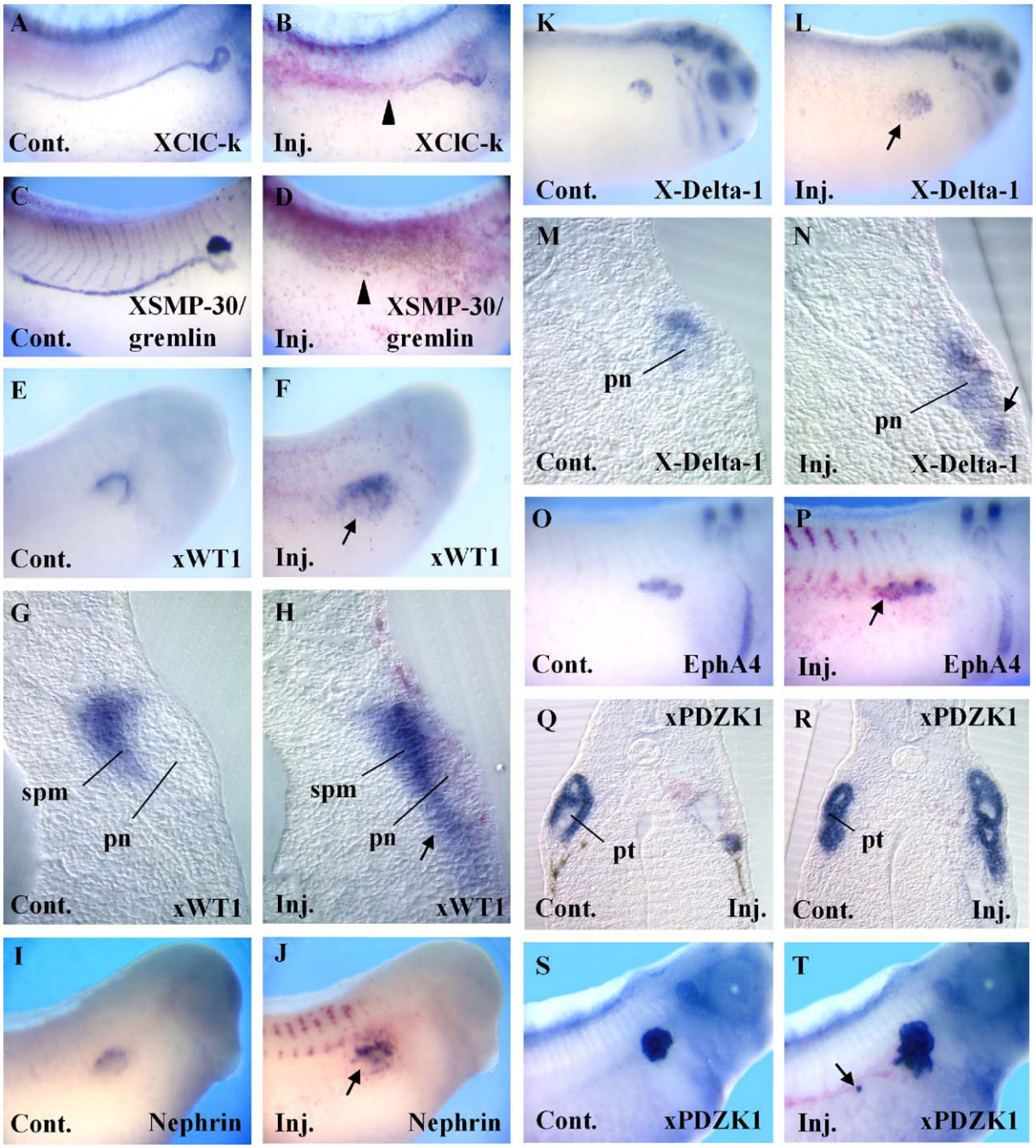

Fig. 8. Overexpression of *Evi1-VP16-hGR* disrupts distal and expands early proximal markers. (A–F, I–L, O–T) Lateral views and (G, H, M, N and Q, R) sections through the pronephros of tailbud or early tadpole stage embryos coinjected with *Evi1-VP16-hGR* mRNA and *β-galactosidase* mRNA and stained with the indicated markers. Control and injected sides marked with Red-gal are shown. Note the inhibition of the expression of the expression of the *XClC-K* (A, B) and *Gremlin* (C, D) distal tubule and duct markers (arrowheads), the expansion of the *xWT1* (E–H) and *nephrin* (I, J) glomus and *X-Delta-1* (K–N) and *EphA4* (O, P) early proximal markers (arrows). (Q) Example of injected embryos with reduced proximal tubules. (R–T) Example of an embryo with a pronephros containing additional tubule branches and ectopic *xPDZK1* staining (arrow). Abbreviations: pn, pronephros; spm, splanchnic layer of the mesoderm; pt, proximal tubules.

VP16 fusion acts as in a dominant negative fashion and that mutation of the corepressor CtBP binding sites inhibits its activity, suggesting that it functions during pronephros development as a transcriptional repressor.

One of the ways Evi1 induces oncogenesis is by blocking TGF-β signaling, which inhibits proliferation of a wide range of cell types. Evi1 directly interacts with Smads through the first zinc finger domain and represses Smads mediated gene activation by recruiting the CtBP corepressor (Palmer et al., 2001; Kurokawa et al., 1998). Our observation that overexpression of Evi1 mutants lacking the first zinc finger domain has no effect either at gastrula stage on *chordin* expression or in the pronephros indicates that Evi1 activity is largely dependent on this ZF1 domain. This raises the

possibility that some of the effects observed in the embryo may be due as recently proposed (Allison et al., 2005) to interference with TGF-β signaling. Interestingly, the BMP antagonist *Gremlin* is expressed like *Evi1* in the pronephric distal tubule and duct (Hsu et al., 1998), suggesting that Evi1 and Gremlin may have overlapping function as TGF-β signaling modulators in pronephros development. In this hypothesis, the lack of effect on BMP dependent genes observed at gastrula stage could be explained by its weaker affinity for Smad1 which relays signals from BMP-activated receptors (Kurokawa et al., 1998; Allison et al., 2005). Alternatively, this could also be independent of TGF-β signaling and due to an essential role of this ZF1 domain in DNA binding. The characterization of downstream target genes for Evi1 is critical to further our understanding of Evi1 function and mode of action in the context of the developing pronephros.

Acknowledgments

We thank Makoto Asashima, Andre Brändli, Mark Fishman, Richard Harland, James Ihle, Chris Kintner, Ryuichi Nishinakamura, Nancy Papalopulu, Roger Patient, Tomas Pieler, Peter Vize and David Wilkinson for providing us with various constructs, and we are grateful to Sadia Kricha for technical assistance. This work was supported by the Belgian program Interuniversitary attraction poles from the Prime Minister's Office, Science Policy Programming (grant P5/35 to E.B. and D.H.), by the Communauté Française de Belgique (grant number ARC 00/05-250 to E.B.), by the Fund for Scientific Medical Research (FRSM 3.4555.01 and 3.4556.01), by the International Brachet Stiftung (grant number 01-4/l) and by the Fondation Reine Elisabeth (grant 11256). C.V.C. was a fellow of the Fonds pour la Formation à la Recherche dans l'Industrie et l'Agriculture.

References

Allison, T., Ko, T.C., Cao, Y., Liang, Y.-Y., Feng, X.-H., Chang, C., Derynck, R., 2005. Repression of BMP and activin-inducible transcription by EVI-1. J. Biol. Chem. 280, 24227–24237.

Aytekin, M., Vinatzer, U., Musteanu, M., Raynaud, S., Wieser, R., 2005. Regulation of the expression of the oncogene EVI1 through the use of alternative mRNA 5′-ends. Genes 356, 160–168.

Bellefroid, E.J., Bourguignon, C., Holleman, T., Ma, Q., Anderson, D.J., Kintner, C., Pieler, T., 1996. X-MyT1, a *Xenopus* C2HC type zinc finger protein with a regulatory function in neuronal differentiation. Cell 87, 1191–1202.

Bellefroid, E.J., Kobbe, A., Gruss, P., Pieler, T., Gurdon, J.B., Papalopulu, N., 1998. Xiro3 encodes a *Xenopus* homolog of the *Drosophila* Iroquois genes and functions in neural specification. EMBO J. 17, 191–203.

Blumberg, B., Bolado, J., Moreno, T.A., Kintner, C., Evans, R.M., Papalopulu, N., 1997. An essential role for retinoid signaling in anteroposterior neural patterning. Development 124, 373–379.

Bradley, L.C., Snape, A., Bhatt, S., Wikinson, D.G., 1993. The structure and expression of the *Xenopus* Krox-20 gene: conserved and divergent patterns of expression in rhombomeres and neural crest. Mech. Dev. 40, 73–84.

Brändli, A.W., 1999. Towards a molecular anatomy of the *Xenopus* pronephric kidney. Int. J. Dev. Biol. 43, 381–395.

Broadbent, J., Read, E.M., 1999. Wholemount in situ hybridization of *Xenopus* and zebrafish embryos. Methods Mol. Biol. 127, 57–67.

Buonamici, S., Li, D., Chi, Y., Zhao, R., Wang, X., Brace, L., Ni, H., Saunthararajah, Y., Nucifora, G., 2004. Evi1 induces myelodysplastic syndrome in mice. J. Clin. Invest. 114, 713–719.

Carroll, T., Vize, P.D., 1996. Wilm's tumor suppressor gene is involved in the development of disparate kidney forms: evidence from expression in the *Xenopus* pronephros. Dev. Dyn. 206, 131–138.

Carroll, T., Vize, P.D., 1999. Synergism between Pax8 and lim-1 in embryonic kidney development. Dev. Biol. 214, 46–59.

Chan, T.-C., Takahashi, S., Asashima, M., 2000. A role for Xlim1 in pronephros development in *Xenopus laevis*. Dev. Biol. 228, 256–269.

Chen, Y., Pollet, N., Niehrs, C., Pieler, T., 2001. Increased XRALDH2 activity has a posteriorizing effect on the central nervous system of *Xenopus* embryos. Mech. Dev. 101, 91–103.

Cheng, H.T., Kopan, R., 2005. The role of Notch signaling in specification of podocyte and proximal tubules within the developing mouse kidney. Kidney Int. 68, 1951–1952.

Cheng, H.T., Miner, J.H., Lin, M., Tansey, M.G., Roth, K., Kopan, R., 2003. γ-Secretase activity is dispensable for mesenchyme-to-epithelium transition but required for podocyte and proximal tubule formation in developing mouse kidney. Development 130, 5031–5042.

Chitnis, A., Henrique, D., Lewis, J., Ish-Horowicz, D., Kintner, C., 1995. Primary neurogenesis in *Xenopus* embryos is regulated by a homologue of the *Drosophila* neurogenic gene Delta. Nature 375, 761–766.

Coffman, C.R., Skoglund, P., Harris, W.A., Kintner, C.R., 1993. Expression of an extracellular deletion of Xotch diverts cell fate in *Xenopus* embryos. Cell 73, 659–671.

Deconinck, A.E., Mead, P.E., Tevosian, S.G., Crispino, J.D., Katz, S.G., Zon, L.I., Orkin, S.H., 2000. FOG acts as a repressor of red blood cell development in *Xenopus*. Development 127, 2031–2040.

Delwel, R., Funabiki, T., Kreider, B.L., Morishita, K., Ihle, J.N., 1993. Four of the seven zinc fingers of Evi-1 myeloid-transforming gene are required for sequence-specific binding to GA(C/T)AAGA(T/C)AAGATAA. Mol. Cell. Biol. 13, 4291–4300.

Drummond, I.A., 2003. Making a zebrafish kidney: a tale of two tubes. Trends Cell Biol. 13, 357–365.

Drummond, I.A., 2005. Kidney development and disease in the zebrafish. J. Am. Soc. Nephrol. 16, 299–304.

Fichelson, S., Dreyfus, F., Berger, R., Melle, J., Bastard, C., Miclea, J.M., Gisselbrecht, S., 1992. Evi-1 expression in leukemic patients with rearrangements of the 3q25–q28 chromosomal region. Leukemia 6, 93–99.

Gammill, L.S., Sive, H., 1997. Identification of otx2 target genes and restrictions in ectodermal competence during *Xenopus* cement gland formation. Development 124, 471–481.

Gerth, V.E., Zhou, X., Vize, P.D., 2005. Nephrin expression and three-dimensional morphogenesis of the *Xenopus* pronephric glomus. Dev. Dyn. 233, 1131–1139.

Grieshammer, U., Cebrian, C., Ilagan, R., Meyers, E., Herzlinger, D., Martin, G. R., 2005. FGF8 is required for cell survival at distinct stages of nephrogenesis and for regulation of gene expression in nascent nephrons. Development 132, 3847–3857.

Hamburger, V., Hamilton, L., 1951. Series of embryonic chicken growth. J. Morphol. 88, 49–92.

Harland, R.M., 1991. In situ hybridization: an improved whole-mount method for *Xenopus* embryos. Methods Cell Biol. 36, 685–695.

Hemmati-Brivanlou, A., de la Torre, J.R., Holt, C., Harland, R.M., 1991. Cephalic expression and molecular characterization of *Xenopus* En-2. Development 111, 715–724.

Hernandez, R., Rikhof, H., Bachmann, R., Moens, C., 2004. vhnf1 integrates global RA patterning and local FGF signals to direct posterior hindbrain development in zebrafish. Development 131, 4511–4520.

Hirai, H., 1999. The transcription factor Evi-1. Int. J. Biochem. Cell Biol. 31, 1367–1371.

Hollemann, T., Chen, Y., Grunz, H., Pieler, T., 1998. Regionalized metabolic activity establishes boundaries of retinoic acid signalling. EMBO J. 17, 7361–7372.

Hoyt, P.R., Bartholomew, C., Davis, A.J., Yutzey, K., Gamer, L.W., Potter, S.S., Ihle, J.N., Mucenski, M.L., 1997. The Evi-1 proto-oncogene is required at midgestation for neural, heart, and paraxial mesenchyme development. Mech. Dev. 65, 55–70.

Hsu, D.R., Economides, A.N., Wang, X., Eimon, P.M., Harland, R.M., 1998. The *Xenopus* dorsalizing factor Gremlin identifies a novel family of secreted proteins that antagonize BMP activities. Mol. Cell 1, 673–683.

James, R.G., Schultheiss, T.M., 2003. Patterning of the avian intermediate mesoderm by lateral plate and axial tissues. Dev. Biol. 253, 109–124.

James, R.G., Schultheiss, T.M., 2005. BMP signaling promotes intermediate mesoderm gene expression in a dose-dependent, cell-autonomous and translation-dependent manner. Dev. Biol. 288, 113–125.

Jones, E.A., 2005. *Xenopus*: a prince among models for pronephric kidney development. J. Am. Soc. Nephrol. 16, 313–321.

Karniski, L.P., Lotscher, M., Fucentese, M., Hilfiker, H., Biber, J., Murer, H., 1998. Immunolocalization of sat-1 sulfate/oxalate/bicarbonate anion exchanger in the rat kidney. Am. J. Physiol. 275, 79–87.

Kazama, H., Kodera, T., Shimizu, S., Mizoguchi, H., Morishita, K., 1999. Ecotropic viral integration site-1 is activated during, and is sufficient for, neuroectodermal P19 cell differentiation. Cell Growth Differ. 10, 565–573.

Kocher, O., Pal, R., Roberts, M., Cirovic, C., Gilchrist, A., 2003. Targeted disruption of the PDZK1 gene by homologous recombination. Mol. Cell. Biol. 23, 1175–1180.

Krieg, P.A., 1991. Synthesis of RNA probes using SP6, T7 and T3 RNA polymerase. Methods Gene Tech. 1, 35–62.

Kurokawa, M., Mitani, K., Irie, K., Matsuyama, T., Takahashi, T., Chiba, S., Yazaki, Y., Matsumoto, K., Hirai, H., 1998. The oncoprotein Evi-1 represses TGF-beta signalling by inhibiting Smad3. Nature 394, 92–96.

Maden, M., 1999. Heads or tails? Retinoic acid will decide. Bioessays 21, 809–812.

Majumdar, A., Lun, K., Brand, M., Drummond, I.A., 2000. Zebrafish no isthmus reveals a role for pax2.1 in tubule differentiation and patterning events in the pronephric primordia. Development 127, 2089–2098.

Marcos-Gutiérrez, C., Wilson, S.W., Holder, N., Pachnis, V., 1997. The zebrafish homologue of the ret receptor and its pattern of expression during embryogenesis. Oncogene 14, 879–889.

Mauch, T.J., Yang, G., Wright, M., Smith, D., Schoenwolf, G.C., 2000. Signals from trunk paraxial mesoderm induce pronephros formation in chick intermediate mesoderm. Dev. Biol. 220, 62–75.

Mavropoulos, A., Devos, N., Biemar, F., Zecchin, E., Argenton, F., Edlund, H., Motte, P., Martial, J.A., Peers, B., 2005. sox4b is a key player of pancreatic alpha cell differentiation in zebrafish. Dev. Biol. 285, 211–223.

Mayor, R., Morgan, R., Sargent, M.G., 1995. Induction of the prospective neural crest of *Xenopus*. Development 121, 767–777.

McLaughin, K.A., Rones, M.S., Mercola, M., 2000. Notch regulates cell fate in the developing pronephros. Dev. Biol. 227, 567–580.

Mochizuki, N., Shimizu, S., Nagasawa, T., Tanaka, H., Tanikawi, M., Yokota, J., Morishita, K., 2000. A novel gene, MEL1, mapped to 1p36.3 is highly homologous to the MDS1/EVI1 gene and is transcriptionally activated in t (1;3)(p36;q21)-positive leukemia cells. Blood 96, 3209–3214.

Morishita, K., Parker, D.S., Mucenski, M.L., Jenkins, N.A., Copeland, N.G., Ihle, J.N., 1988. Retroviral activation of a novel gene encoding a zinc finger protein in IL-3-dependent myeloid leukemia cell lines. Cell 54, 831–840.

Morishita, K., Parganas, E., Parham, D.M., Matsugi, T., Ihle, J.N., 1990. The Evi-1 zinc finger myeloid transforming gene is normally expressed in the kidney and in developing oocytes. Oncogene 5, 1419–1423.

Morishita, K., Suzukawa, K., Taki, T., Ihle, J.N., Yokota, J., 1995. Evi-1 zinc finger protein works as a transcriptional activator via binding to a consensus sequence GACAAGATAAGATAAN $_{1-28}$ CTCATCTTC. Oncogene 10, 1961–1967.

Mucenski, M.L., Taylor, B.A., Ihle, J.N., Hartley, J.W., Morse III, H.C., Jenkins, N.A., Copeland, N.G., 1988. Identification of a common ecotropic viral integration site, Evi-1, in the ADN of AKXD murine myeloid tumors. Mol. Cell. Biol. 8, 301–308.

Nakai, S., Sugitani, Y., Sato, H., Ito, S., Miura, Y., Ogawa, M., Nishi, M., Jishage, K.-I., Minowa, O., Noda, T., 2003. Crucial roles of Brn1 in distal tubule formation and function in mouse kidney. Development 130, 4751–4759.

Nieto, M.A., Bradley, L.C., Wilkinson, D.G., 1991. Conserved segmental expression of Krox-20 in the vertebrate hindbrain and its relationship to lineage restriction. Development Suppl. 2, 59–62.

Nieuwkoop, P.D., Faber, J., 1997. A Normal Table of *Xenopus laevis* (Daudin). North Holland Publishing Co, Amsterdam, The Netherlands.

Nishikata, I., Sasaki, H., Tateno, Y., Imayoshi, S., Asou, N., Nakamura, T., Morishita, K., 2003. A novel EVI1 gene family, MEL1, lacking a PR domain (MEL1S) is expressed mainly in t(1;3)(p36;q21)-positive AML and blocks G-CSF-induced myeloid differentiation. Blood 102, 3323–3332.

Obara-Ishihara, T., Kuhlman, T., Niswander, L., Herzlinger, D., 1999. The surface ectoderm is essential for nephric duct formation in intermediate mesoderm. Development 126, 1103–1108.

Osafune, K., Nishinakamura, R., Komazaki, S., Asashima, M., 2002. In vitro induction of the pronephric duct in *Xenopus* explants. Dev. Growth Differ. 44, 161–167.

Palmer, S., Brouillet, J.-P., Kilbey, A., Fulton, R., Walker, M., Crossley, M., Bartholomew, C., 2001. Evi-1 transforming and repressor activities are mediated by CtBP co-repressor proteins. J. Biol. Chem. 276, 25834–25840.

Perkins, A.S., Mercer, J.A., Jenkins, N.A., Copeland, N.G., 1991. Patterns of Evi-1 expression in embryonic and adult tissues suggest that Evi-1 plays an important regulatory role in mouse development. Development 111, 479–487.

Ruiz i Altaba, A., Jessell, T., 1991. Retinoic acid modifies mesodermal patterning in early *Xenopus* embryos. Genes Dev. 5, 175–187.

Ryan, K., Butler, K., Bellefroid, E., Gurdon, J.B., 1998. *Xenopus* eomesodermin is expressed in neural differentiation. Mech. Dev. 75, 155–158.

Ryffel, G.U., 2003. What can a frog tell us about kidney development. Nephron. Exp. Nephrol. 94, 35–43.

Sasai, Y., Lu, B., Steinbeisser, H., Geissert, D., Gont, L.K., De Robertis, E.M., 1994. *Xenopus* chordin: a novel dorsalizing factor activated by organizer-specific homeobox genes. Cell 79, 779–790.

Sato, A., Asashima, M., Yokota, T., Nishinakamura, R., 2000. Cloning and expression pattern of a *Xenopus* pronephros-specific gene, XSMP-30. Mech. of Dev. 92, 273–275.

Serluca, F.C., Fishman, M.C., 2001. Pre-pattern in the pronephric kidney field of zebrafish. Development 128, 2233–2241.

Seufert, D.W., Brennan, H.C., DeGuire, J., Jones, E.A., Vize, P.D., 1999. Developmental basis of pronephric defects in xenopus body plan phenotypes. Dev. Biol. 215, 233–242.

Smith, J.C., Price, B.M., Green, J.B., Weigel, D., Herrmann, B.G., 1991. Expression of a *Xenopus* homolog of Brachyury (T) is an immediate-early response to mesoderm induction. Cell 67, 79–87.

Smith, A., Robinson, V., Patel, K., Wilkinson, D.G., 1997. The EphA4 and EphB1 receptor tyrosine kinase and ephrin-B2 ligand regulate targeted migration of branchial neural crest cells. Curr. Biol. 7, 561–570.

Taira, M., Otani, H., Saint-Jeannet, J., Dawid, I., 1994. Role of the LIM class homeodomain protein Xlim-1 in neural and muscle induction by the Spemann organizer in *Xenopus*. Nature 372, 677–679.

Turner, D.L., Weintraub, H., 1994. Expression of achaete–scute homolog 3 in *Xenopus* embryos converts ectodermal cells to a neural fate. Genes Dev. 8, 1434–1447.

Vize, P.D., 2003. The chloride conductance channel ClC-K is a specific marker for the *Xenopus* pronephric distal tubule and duct. Gene Expression Patterns 3, 347–350.

Vize, P.D., Seufert, D.W., Carroll, T.J., Wallingford, J.B., 1997. Model systems for the study of kidney development: use of the pronephros in the analysis of organ induction and patterning. Dev. Biol. 188, 189–204.

Vize, P.D., Woolf, A.S., Bard, J.B.L., 2003. The Kidney. From Normal Development to Congenital Disease. Academic Press, Amsterdam.

Wallingford, J.B., Carroll, T.J., Vize, P.D., 1998. Precocious expression of the Wilm's tumor gene xWT1 inhibits embryonic kidney development in *Xenopus laevis*. Dev. Biol. 202, 103–112.

Wang, P., Pereira, F.A., Beasley, D., Zheng, H., 2003. Preselinins are required for the formation of comma- and S-shaped bodies during nephrogenesis. Development 130, 5019–5029.

Wettstein, D.A., Turner, D.L., Kintner, C., 1997. The *Xenopus* homolog of *Drosophila* Suppressor of Hairless mediates Notch signaling during primary neurogenesis. Development 124, 693–702.

Wilkinson, D.G., Nieto, M.A., 1993. Detection of messenger RNA by in situ hybridization to tissue sections and whole mounts. Methods Enzymol. 225, 361–373.

Yuasa, H., Oike, Y., Iwama, A., Nishikata, I., Sugiyama, D., Perkins, A., Mucenski, M.L., Suda, T., Morishita, K., 2005. Oncogenic transcription factor Evi1 regulates hematopoietic stem cell proliferation through GATA-2 expression. EMBO J. 24, 1976–1987.

Zhou, X., Vize, P.D., 2004. Proximo-distal specialization of epithelial transport processes within the *Xenopus* pronephric kidney tubules. Dev. Biol. 271, 322–338.

Zon, L., Mather, C., Burgess, S., Bolce, M., Harland, R., Orkin, S., 1991. Expression of GATA-binding proteins during embryonic development in *Xenopus laevis*. Proc. Natl. Acad. Sci. U. S. A. 88, 10642–10646.